

SCALAR WAVES IN SPACETIMES WITH CLOSED TIMELIKE CURVES

NECMİ BUĞDAYCI

DECEMBER 2005

SCALAR WAVES IN SPACETIMES WITH CLOSED TIMELIKE CURVES

A THESIS SUBMITTED TO
THE GRADUATE SCHOOL OF NATURAL AND APPLIED SCIENCES
OF
THE MIDDLE EAST TECHNICAL UNIVERSITY

BY

NECMİ BUĞDAYCI

IN PARTIAL FULFILLMENT OF THE REQUIREMENTS FOR THE DEGREE
OF
IN PARTIAL FULLFILLMENT OF THE REQUIREMENTS FOR THE
DEGREE DOCTOR OF PHILOSOPHY
IN
PHYSICS

DECEMBER 2005

Approval of the Graduate School of Natural and Applied Sciences

Prof. Dr. Canan Özgen
Director

I certify that this thesis satisfies all requirements as a thesis for the degree of Doctor of Philosophy

Prof. Dr. Sinan Bilikmen
Head of Department

This is to certify that we have read this thesis and that in our opinion it is fully adequate, in scope and quality, as a thesis for the degree of Doctor of Philosophy.

Prof. Dr. Sibel Başkal
Supervisor

Examining Committee Members

Prof. Dr. Cem Tezer (METU, Math.)	_____
Prof. Dr. Sibel Başkal (METU, Phys.)	_____
Prof. Dr. Erhan Onur İltan (METU, Phys)	_____
Prof. Dr. Mustafa Savcı (METU, Phys)	_____
Assoc.Prof. Dr. Dumitru Balenau (Çankaya Univ.)	_____

I hereby declare that all information in this document has been obtained and presented in accordance with academic rules and ethical conduct. I also declare that, as required by these rules and conduct, I have fully cited and referenced all material and results that are not original to this work.

Name, Last name : Necmi Buğdaycı

Signature :

ABSTRACT

SCALAR WAVES IN SPACETIMES WITH CLOSED TIMELIKE CURVES

Necmi Buğdaycı

Ph. D., Department of Physics

Supervisor: Prof. Dr. Sibel Başkal (METU, Phys.)

December 2005, 60 pages

The existence and -if exists- the nature of the solutions of the scalar wave equation in spacetimes with closed timelike curves are investigated. The general properties of the solutions on some class of spacetimes are obtained.

Global monochromatic solutions of the scalar wave equation are obtained in flat wormholes of dimensions $2+1$ and $3+1$. The solutions are in the form of infinite series involving cylindrical and spherical wave functions and they are elucidated by the multiple scattering method. Explicit solutions for some limiting cases are produced as well. The results of $2+1$ dimensions are verified by using numerical methods.

Keywords:

Wave Equation, Helmholtz Equation, Wormhole Spacetimes, Closed Timelike Curves, Non-Globally Hyperbolic Spacetimes, Bessel functions, Addition Theorems, Spherical Waves..

ÖZ

KAPALI ZAMANSAL EĞRİLER İÇEREN UZAYZAMANLARDA SKALER DALGALAR

Necmi Buğdaycı

Doktora, Fizik Bölümü

Tez Yöneticisi: Prof. Dr. Sibel Başkal (METU, Phys.)

Aralık 2005, 60 sayfa

Kapalı zamansal eğriler içeren uzay-zamanlarda varolabilecek dalgaların doğası araştırılmaktadır. Bu sınıfa giren uzay-zamanların belli bazı türlerinde dalga denkleminin çözümlerinin karakteristik özellikleri elde edilmiştir.

2+1 ve 3+1 boyutlu düz solucan deliği uzayzamanlarda dalga denkleminin global çözümleri bulunmuştur. Çözümler silindirik ve küresel Bessel fonksiyonları cinsinden sonsuz seri toplamı olarak ifade edilmiş ve çoklu saçılım yöntemiyle hesaplanmışlardır. Bazı limit durumlar için açık çözümler verilmiş, ayrıca 2+1 boyutta elde edilen çözümler sayısal yöntemler kullanılarak doğrulanmıştır.

Anahtar Kelimeler:

Dalga denklemi, Helmholtz denklemi, solucan-deliği uzay-zamanları, Kapalı zamansal eğriler, Global hiperbolik olmayan uzay-zamanlar, Bessel fonksiyonları, toplama teoremleri, küresel dalgalar

ACKNOWLEDGEMENTS

The author wishes to thank his supervisor Prof. Dr. Sibel Başkal for her guidance and Prof. Dr. Cem Tezer for his helpful discussions throughout the research.

TABLE OF CONTENTS

PLAGIARISM	iii
ABSTRACT	iv
ÖZ	v
ACKNOWLEDGEMENTS	vi
CHAPTER	
1 INTRODUCTION	1
2 GENERAL RESULTS ON SOME CLASS OF SPACE-	
TIMES ADMITTING CLOSED TIMELIKE CURVES	6
2.1 Spacetimes that are compact in Time direction:	6
2.2 Spacetimes of trivial topology with metric tensors admitting closed	
timelike curves:	8
2.2.1 2+1 dimensional sample spacetimes	8
2.2.2 Gödel's universe:	13
3 SCALAR WAVES IN A WORMHOLE SPACETIME ..	15
3.1 Flat wormhole	15
3.2 2+1 Dimensions:	18
3.2.1 Solutions for $a \ll d$ and $a \ll 1$:	24
3.2.2 Multiple scattering	27
3.3 3+1 Dimensions	30

3.4	Numerical verification of the solution:	39
3.5	Dependence of the scattered waves to wormhole parameters	45
3.6	Comparison with the scattering from a conducting cylinder:	47
4	CONCLUSIONS	54
	REFERENCES	57
	APPENDIX	61
	VITA	64

LIST OF FIGURES

2.1	Null cones of M^t	9
2.2	Null cones of M^r	9
2.3	Null cones of M^θ	10
2.4	Variation of timelike direction with r	12
3.1	2+1 dimensional flat wormhole. P is identified with Q. Arrows indicate the direction of the identification.	16
3.2	Coordinates used for 2+1 dimensions.	18
3.3	Coordinates used for 3+1 dimensions.	30
3.4	The contour plot of $\text{Re}(\Psi - e^{i\omega\tau} R\Psi)$ in the vicinity of left wormhole mouth Δ_- . The contour circle at $r = a$ shows that $(\Psi - e^{i\omega\tau} R\Psi) _{r=a}$ is constant. ($\omega a = 20$; $\omega d = 120$; $\tau = 1$; $\alpha = \pi/3$)	40
3.5	The contour plot of $\text{Re}(\frac{\partial}{\partial r}(\Psi + e^{i\omega\tau} R\Psi))$ in the vicinity of left wormhole mouth Δ_- . The same contour circle at $r = a$ is evident. ($\omega a = 20$; $\omega d = 120$; $\tau = 1$; $\alpha = \pi/3$)	41
3.6	The contour plot of $\text{Re}(\Psi)$ in the vicinity of Δ_- . The incident wave is coming from the left with an angle $\pi/3$ and the shadow is on the opposite side. ($\omega a = 20$; $\omega d = 120$; $\tau = 1$; $\alpha = \pi/3$).	42
3.7	Comparison of the multiple scattering and the iteration results. The difference of $ B_n $ found by these two methods are points with marker 'x' which are zero for all n . ($\omega a = 20$; $\omega d = 120$; $\tau = 1$; $\alpha = \pi/3$)	43
3.8	Comparison of the multiple scattering and the $a \ll d$ approximation. ($\omega a = 5$; $\omega d = 1600$; $\omega\tau = 1$; $\alpha = \pi/5$)	44
3.9	Scattering coefficients for different $\omega\tau$ values: From above to below $\omega\tau$ values are π , $\pi/2$ and 0, respectively. ($\omega a = 15$, $\omega d = 200$, $\alpha = 0$).	46
3.10	From above to below, $\omega\tau$ values are again π , $\pi/2$ and 0, respectively. ($\omega a = 60$, $\omega d = 180$, $\alpha = 0$).	47
3.11	$\alpha = \pi/3$. $\omega\tau$ values are again π , $\pi/2$ and 0, respectively from above to below. ($\omega a = 30$, $\omega d = 300$).	48

3.12	The Contour plot of the total wave around left wormhole mouth for $\omega\tau = 0$. ($\omega a = 15$, $\omega d = 40$, $\alpha = 0$)	49
3.13	The Contour plot of the total wave around left wormhole mouth for $\omega\tau = \pi/2$. ($\omega a = 15$, $\omega d = 40$, $\alpha = 0$)	50
3.14	The Contour plot of the total wave around left wormhole mouth for $\omega\tau = \pi$. The effect of the shadow at upper part of the wormhole mouth shows itself stronger than othe $\omega\tau$ values. ($\omega a = 15$, $\omega d = 40$, $\alpha = 0$)	51
3.15	Below: $\omega a = 15, \omega d = 1600$; above: $\omega a = 15, \omega d = 30.02$. ($\alpha = 0$) . . .	52
3.16	From above to below, $\omega d = 500$, $\omega d = 200$, $\omega d = 50$ and $\omega d = 42$ respectively. ($\omega a = 15$, $\alpha = \pi/3$).	52
3.17	From above to below: (1) conducting sphere. (2) wormhole: $\omega\tau = \pi$; (3) wormhole: $\omega\tau = 0$; ($\omega a = 20$, $\omega d = 80$, $\alpha = 0$)	53

CHAPTER 1

INTRODUCTION

In this thesis, the effect of existence of closed timelike curves on the solutions of scalar wave equation is investigated. The main motivation is the problematic nature of the closed timelike curves -which results from their causality violating property- in physics . It is investigated whether this problematic nature shows itself in the waves propagating in this kind of spacetimes.

In spacetimes admitting closed timelike curves, it is possible to travel to the past as time propagates in future direction. Therefore closed timelike curves can be interpreted as time-machines. This means past and future are not separated from each other. A point on such a spacetime can be both at the chronological future, and at the chronological past of another point. Causality issues arise due to this property, and the classical cause and effect relation between events are no longer definite.

Existence of closed timelike curves contradicts with the strong belief of common sense which states that there exists only one copy of an object in the space at a specific time. Following a timelike curve in future direction, if an object may return infinitesimally close to its original spacetime point, a local observer will be able to observe two instances of the same object at the same time.

Another questionable issue regarding to the closed timelike curves is the common notion of free will. It is customary to believe that the past has passed away and cannot be changed anymore, but we can effect the future by our intentional behaviors. In a universe where closed timelike curves can exist, the future and the past are not distinguishable from each other. In such a spacetime either one has no control on future which means there is no free will, or one can change the past with his actions at present time. This second alternative falls into a logical contradiction

called grandfather paradox. By changing the past from present time, the conditions that created present time would be altered, hence present time would not be the same. Therefore the person that changes the past through his actions would not exist in present time.

The entropy law is still another problem regarding time travel physics. According to second law of thermodynamics, entropy always increases with time which flows in one direction, namely future direction. Therefore past and future is clearly distinguishable in terms of entropy, and a spacetime where past and future are interchangeable contradicts with the entropy law.

Despite all these paradoxes and unreasonable consequences, there is no law forbidding the chronology violating spacetimes within the context of general relativity. Einstein field equations, which are the main equations of General Relativity theory, put no restriction on the causal structure of the spacetime. The chronology violating spacetimes, may violate the so called "energy conditions". However energy conditions are not physical laws, they are just conjectures that universe believed by most of the physicists to obey.

In the mathematical structure of General Relativity, time and space coordinates are distinguished from each other by means of a minus sign present in the Lorentzian metric of the spacetime. Also the fact (which is apparent from everyday experience) that time is in continuous flow, and locally every moment is lived only once, is accommodated in relativity theory by postulating that every particle follows a time-like curve in spacetime. Except these two differences, the role of time and space is symmetric the framework of General relativity. If it is possible to find out the mathematical anomalies/inconsistencies of chronology violating spacetimes within the boundaries of current physics, the mathematical tools we have are the unique time direction of the Lorentzian spacetime and the timelike curves.

In this context the waves propagating in chronology violating universes are worth to study. If we can find out the some characteristic common properties of the solutions of the wave equation in the chronology violating spacetimes, at least theoretically, this can be used to get a clue about whether our universe admits closed timelike curves and time travel.

For simplicity, only homogenous classical scalar wave equation is considered. The

theory of tensor wave equations is closely related to that of scalar wave equations and can be considered only a simple extension of it [1]. Therefore solutions of vector (or more generally tensor) wave equations are not expected to have significantly different qualitative properties from solutions of the scalar wave equation.

Throughout the thesis, a spacetime (M, g, D) will be defined as "a connected, oriented and time oriented Lorentzian manifold (M, g) together with the Levi-Civita connection D of g on M " [2] [3]. With this definition, the universe models that admit more than one timelike direction are excluded since they fail to be Lorentzian. Gödel's universe which admits two timelike direction (and therefore not Lorentzian) is an exception which is considered in section II. On the other hand the dimension is not required to be four and different dimensional spacetimes will be allowed in order to investigate the effect of closed timelike curves in simpler lower dimensional models.

In chapter 2, general properties of the solutions of wave equation on some class of spacetimes are studied. It is very difficult to find out general rules (if there exist any) that are valid for all spacetimes that admit closed timelike curves. What determines the causal character of a spacetime is (1) its topology and (2) its metric tensor. In section 2.1, a class of spacetimes are treated in which existence of closed timelike curves are a natural consequence of the their topology. These spacetimes are compact in time direction and closed timelike curves exist globally all over the spacetime. The characteristic property of these solutions is that their frequency spectrum are a discrete set instead of continuum. This brings a severe restriction on the solution set. However the same type of restriction is also present for the globally hyperbolic spacetimes when the space dimensions form a compact manifold.

In section 2.2 manifolds of more trivial topology $(\mathbb{R}^n$ or $(\mathbb{R}^{n-1} - \{0\}) \times \mathbb{R})$ are considered. In these class of spacetimes, the tip of the null cone changes direction in time and bends to make a close loop. Suitable metric tensors are written for these spacetimes and separation of variables is used to obtain the solutions. Godel's universe is also discussed as an example of the same kind of manifold.

It is remarkable that again in these kind of spacetimes, only a discrete set of frequencies are allowed as solutions of the wave equation.

Chapter 3 is dedicated to wormholes, in particular 2+1 and 3+1 dimensional

flat wormholes. As a significant consequence of their non-trivial topology, wormholes also admit closed timelike curves (CTC's). As such they constitute a suitable framework for the study of the solutions of the scalar wave equation in a spacetime admitting closed timelike curves.

Due to the topology of a wormhole, no single coordinate chart is sufficient to express the global geometry of the whole wormhole spacetime and it becomes necessary to develop techniques to handle global issues on the one hand and to investigate the propagation of scalar waves near closed timelike curves. It should be mentioned that there are works that study the scalar and electromagnetic waves that are valid locally in a certain region (such as may be termed the “throat”) of the wormhole or that study waves in similar spacetimes [4],[5],[6],[7],[8],[9],[10].

Wormholes are widely studied and discussed, especially after the paper of Morris and Thorne, in the context of time travel [11],[12],[13],[14],[15],[16]. Cauchy problem of the scalar wave equation in the flat wormhole considered here is studied throughout by Friedman and Morris with a variety of other spacetimes admitting closed timelike curves [17],[18]. They also proved that there exist a unique solution of Cauchy problem for a class of spacetimes, including our case, with initial data given at past null infinity [19].

Due to the wormhole structure, the boundary conditions imposed in solving the Helmholtz equation depends on the frequency. Therefore spectral theorem is not applicable in a straight forward manner to express the solution of the wave equation as a superposition of monochromatic wave solutions. However, in [19], it is proved using limiting absorption method that, the superpositions of the monochromatic wave solutions of the problem converge to the solution of wave equation.

The problem can be handled as a Cauchy problem with given initial data at past null infinity or alternatively as a scattering problem, i.e. finding scattered waves from the wormhole handle for a given incident wave.

The approach used in section III is similar to that used in scattering from infinite parallel cylinders [20]. Ψ_1 and Ψ_2 represents outgoing cylindrical (for 3+1 dimensions spherical) waves emerging from the first and the second wormhole mouth respectively. In order to be able to apply the boundary conditions conveniently which arise from the peculiar topology of the wormhole in our case, it is necessary

to express Ψ_1 in terms of cylindrical (spherical) waves centered at second mouth and vice versa. Addition theorems for cylindrical and spherical wave functions are employed for this purpose.

The equations for the scattering coefficients of Ψ_1 and Ψ_2 that result from the boundary conditions in question are in general not amenable to direct algebraic manipulation . The multiple scattering method is applied to obtain an infinite series solution. On the other hand for some important limiting cases the equations solved explicitly. The solutions by these both methods are consistent with one another.

In section 3.1, the spacetime is described and the general formulation of the problem is presented. In section 3.2, 2+1 dimensional case is studied. The equations are presented, explicit solutions for two limiting cases are obtained, and finally the multiple scattering solution is applied. In Section 3.3, the same scheme as section 3.2 is followed for 3+1 dimensional case. In section 3.4 numerical verifications of the results obtained in section 3.2 are presented. In section 3.5 the solution for different wormhole parameters are presented and finally in section 3.6 the scattering coefficients of the wormhole is compared with that of scattering from a infinite conducting cylinder.

CHAPTER 2

GENERAL RESULTS ON SOME CLASS OF SPACETIMES ADMITTING CLOSED TIMELIKE CURVES

2.1 Spacetimes that are compact in Time direction:

The existence of closed timelike curves in a spacetime emerges in different ways. One class of spacetimes that admit closed timelike curves are those spacetimes which are compact in time direction. The generic topology for this kind of spacetimes can be considered as $M \times S^1$ where M is an arbitrary Riemannian manifold. In this class of spacetimes, time is vicious. Every timelike curve advancing to future returns back to past after some time.

Every non-compact manifold admits some Lorentzian metric defined on it, however this is not true in general for compact manifolds [21]. Some compact manifolds does not admit Lorentzian metric, and hence they are excluded from being spacetime according to our definition. The simplest examples of this kind are S^4 and $S^2 \times S^2$. The manifolds considered in this section are product manifolds and they are compact iff both manifolds entering to the product are compact. For the spacetimes analyzed here, one of the manifolds entering the product is one dimensional representing the time direction. Although not every compact manifold admit a Lorentzian metric defined on it, all compact manifolds of product type where one of the products is

one dimensional manifold and represent the timelike direction, admits some Lorentz metric defined on it.

If the metric is flat in such a cylindrical spacetime, it is well known that the possible wave solutions are limited to certain discrete frequencies. An important question is whether this restriction is a result of existence of closed timelike curves. The compactness of the spacetime manifold in space direction may result exactly the same kind of restriction on solutions of wave equation.

Consider a spacetime manifold $\hat{M} = M \times N$ where M is a Riemannian 3 manifold and N is an one dimensional Riemannian manifold. The metric of the product spacetime is considered not to be warped, i.e., in the expression of the metric tensor, the coefficients of time variable $dt \otimes dt$ is independent of space variables \vec{x} , and coefficient of $d\vec{x} \otimes d\vec{x}$ is independent of t . In this case it is natural to assume a solution that is separable into time and space coordinates:

Let $F : \hat{M} \rightarrow \mathbb{C}$, $u : M \rightarrow \mathbb{C}$ and $v : N \rightarrow \mathbb{C}$ be functions on \hat{M} , M and N .

$$F(x, t) = u(x)v(t) \quad (2.1.1)$$

$$\Delta F = \Delta u(x)v(t) - u(x)\Delta v(t) = 0 \quad (2.1.2)$$

2.1.2 gives two equations for $u(x)$ and $v(t)$:

$$\Delta u_\lambda(x) = \lambda u_\lambda(x) \quad (2.1.3)$$

$$\Delta v_\lambda(t) = \lambda v_\lambda(t) \quad (2.1.4)$$

The solution of 2.1.4 is:

$$u(t) = e^{i\lambda t} \quad (2.1.5)$$

Therefore the eigenvalues λ are indeed the frequencies of monochromatic wave solutions to the wave equation on \hat{M} .

Given any compact Riemannian manifold, it is well known that the eigenvalues

of Laplacian Δ , forms a discrete set [22]. Thus if N is compact, $\lambda = \omega_n$, $n \in \mathbb{Z}$. Therefore there is solution to wave equation only for discrete frequencies.

On the other hand the same result applies also to M . If M is compact, 2.1.3 has discrete eigenvalues and again $\lambda = \omega_n$, $n \in \mathbb{Z}$.

If both M and N are compact, the solution set has the common elements of the set of eigenvalue of 2.1.3 and 2.1.4. If the intersection of the eigenvalue sets is empty, there is no non-constant solution for wave equation. Similar method of separation of variables can be extended to warped product manifolds [23].

A simple example of a spacetime which is compact in either directions is a two dimensional torus spacetime given in [17]. In this case the eigenvalues of 2.1.3 are $\frac{2\pi m}{L}$, $m \in \mathbb{Z}$, where L is the length of the torus in space dimensions and eigenvalues of 2.1.4 are $\frac{2\pi n}{T}$, $n \in \mathbb{Z}$, where T is the length in time direction. Therefore a non-constant solution exists only when $\frac{2\pi m}{L} = \frac{2\pi n}{T}$. Therefore there exist no solution when $\frac{L}{T}$ is irrational.

This simple example suggests that the effect of closed timelike curves does not have a distinguishable effect on solutions of the wave equation.

2.2 Spacetimes of trivial topology with metric tensors admitting closed timelike curves:

Closed timelike curves can also appear in manifolds of topology \mathbb{R}^n . The metric of the spacetime can be adjusted such that the tip of the null cone deflects and make a loop. One simplest way of producing closed timelike curves is to assign the angular coordinate θ direction to be timelike direction in a cylindrical coordinate system (r, θ, t) where $\theta = 0$ and $\theta = 2\pi$ is identified.

2.2.1 2+1 dimensional sample spacetimes

Consider the spacetime $M = (\mathbb{R}^2 - \{0\}) \times \mathbb{R}$ and the cylindrical coordinates system (r, θ, t) defined on it. In usual flat Minkowski spacetime, the tip of the null

cone always points the t direction. When the time direction is chosen as θ , there exist closed timelike curves. Alternatively time direction can be chosen as r which does not admit closed timelike curves either. These spacetimes will be denoted by M^t , M^θ and M^r , respectively.

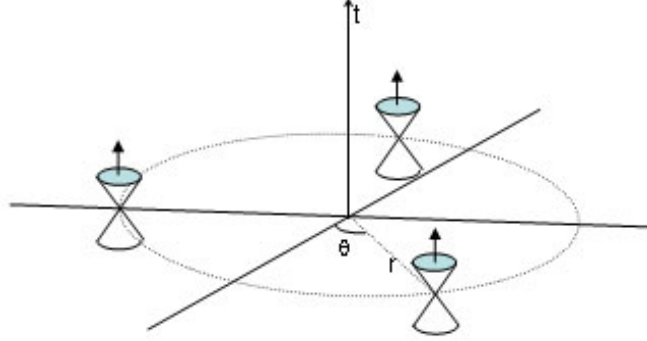


Figure 2.1: Null cones of M^t

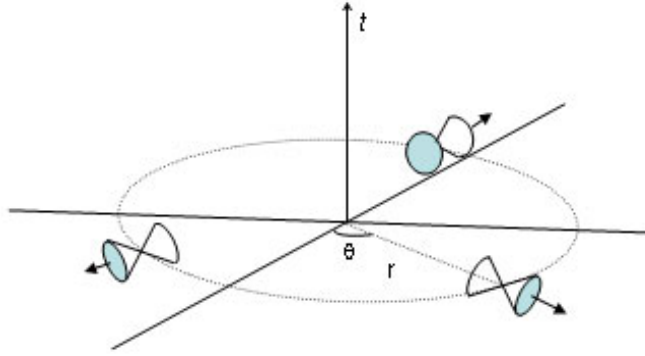


Figure 2.2: Null cones of M^r

The metric tensor in (r, θ, t) coordinates for M^t is

$$g_{ij}dx^i dx^j = dr^2 + r^2 d\phi^2 - dt^2 \quad (2.2.6)$$

The homogenous wave equation for a general metric is:

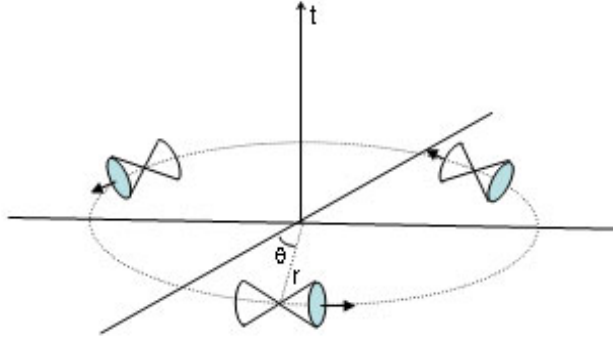


Figure 2.3: Null cones of M^θ

$$\Delta F = \frac{1}{\sqrt{|\det(g_{ij})|}} \frac{\partial}{\partial x^i} (\sqrt{|\det(g_{ij})|} g^{ij} \frac{\partial F}{\partial x^j}) = 0 \quad (2.2.7)$$

Since the metric coefficients are independent of t and θ , it is natural to separate the variables in t and θ direction and assume a solution of the type:

$$F(r, \theta, t) = u(r) e^{im\theta} e^{-i\omega t} \quad (2.2.8)$$

Periodicity of θ with 2π forces m to be an integer. The resulting equation

$$\frac{d^2}{dr^2} u(r) + \frac{1}{r} \frac{d}{dr} u(r) + (\omega^2 - \frac{m^2}{r^2}) u(r) = 0 \quad (2.2.9)$$

is the famous Bessel's differential equation with solution:

$$u(r) = J_m(\omega r) \quad (2.2.10)$$

$$F(r, \theta, t) = J_m(\omega r) e^{im\theta} e^{-i\omega t} \quad (2.2.11)$$

For M^r the metric tensor is:

$$g_{ij} dx^i dx^j = -dr^2 + r^2 d\phi^2 + dt^2 \quad (2.2.12)$$

and the differential equation for r is:

$$\frac{d^2}{dr^2}u(r) + \frac{1}{r}\frac{d}{dr}u(r) + (\omega^2 + \frac{m^2}{r^2})u(r) = 0 \quad (2.2.13)$$

The solution to 2.2.13 is again in terms of Bessel functions, but this time with imaginary order:

$$F(r, \theta, t) = J_{im}(\omega r)e^{im\theta}e^{-i\omega t} \quad (2.2.14)$$

Finally the metric and radial equation for M^θ are:

$$g_{ij}dx^i dx^j = dr^2 - r^2 d\phi^2 + dt^2 \quad (2.2.15)$$

$$\frac{d^2}{dr^2}u(r) + \frac{1}{r}\frac{d}{dr}u(r) + (\omega^2 + \frac{m^2}{r^2})u(r) = 0 \quad (2.2.16)$$

and the solution reads:

$$F(r, \theta, t) = J_{im}(i\omega r)e^{im\theta}e^{-i\omega t} \quad (2.2.17)$$

The Bessel function can be generalized for complex order and complex argument [24]. The solutions for M^θ and M^r are expressed in terms of these Bessel functions of imaginary order and imaginary argument in (2.2.14) and (2.2.17).

For M^θ , since timelike direction is θ , m can be interpreted as frequency, and it is discrete. Therefore only discrete frequencies can propagate in this kind of a spacetime. It is noteworthy that, the restriction on the solution of the wave equation is the same with that of spacetimes that are compact in time direction.

A more general class of spacetimes can be defined that have closed timelike curves in certain region of the spacetime. Consider \mathbb{R}^3 equipped with the metric in cylindrical coordinates as:

$$g_{ij}dx^i dx^j = dr^2 + \cos(2\alpha(r))r^2 d\theta^2 - \cos(2\alpha(r))dt^2 - 2\sin(2\alpha(r))dt d\theta \quad (2.2.18)$$

where $\theta = 0$ is identified with $\theta = 2\pi$.

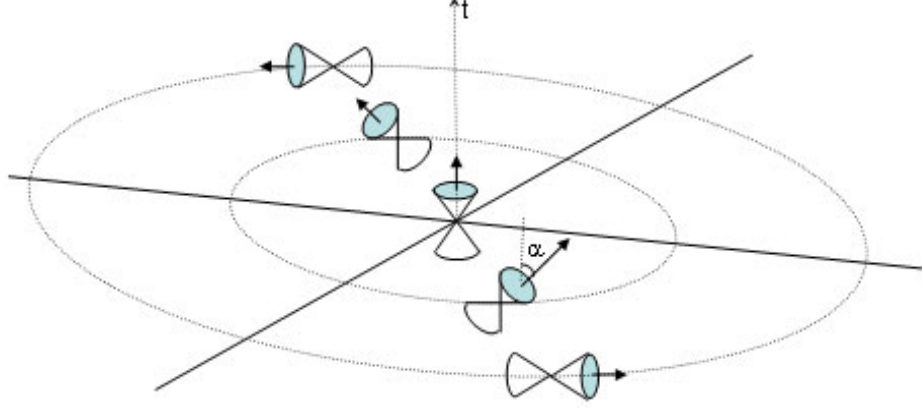


Figure 2.4: Variation of timelike direction with r

The orientation of null cone for this type of metric is shown in the figure 2.4. When $r = 0$, null cone is indefinite unless $\alpha(0) = 0$. Therefore $\alpha(r)$ will be chosen to satisfy $\alpha(0) = 0$.

When $\alpha(r) < \pi/4$ for all r , there exist no closed timelike or null curves. When $\pi/4 < \alpha(r) < 3\pi/4$, time coordinate is not t anymore; instead θ is the time coordinate. Since θ coordinate is cyclic with period 2π , closed timelike curves exist in this case.

Homogenous wave equation in for this metric is:

$$\frac{1}{r} \left(\frac{\partial}{\partial r} r \frac{\partial F}{\partial r} \right) + \frac{\cos(2\alpha)}{r^2} \frac{\partial^2 F}{\partial \theta^2} - \cos(2\alpha) \frac{\partial^2 F}{\partial t^2} - \frac{2}{r} \sin(2\alpha) \frac{\partial^2 F}{\partial \theta \partial t} = 0 \quad (2.2.19)$$

Again the separation of variables in θ and t can be used:

$$F(t, r, \theta) = e^{-i\omega t} e^{ik_1 \theta} u(r) \quad (2.2.20)$$

2.2.19 gives:

$$\frac{d^2}{dr^2}u(r) + \frac{1}{r}\frac{d}{dr}u(r) + [(\omega^2 - \frac{m^2}{r^2})\cos(2\alpha) + \frac{2m\omega}{r}\sin(2\alpha)]u(r) = 0 \quad (2.2.21)$$

For $|\alpha(r)| < \pi/4$, or $|\pi - \alpha(r)| < \pi/4$, timelike direction is t , and ω represents the frequency. However, when $\pi/4 \leq \alpha(r) \leq 3\pi/4$ since timelike direction is switched to be θ , k_1 represents the frequency of the wave.

Periodicity of θ with 2π requires k_1 to be an integer: $k_1 = m$, $m \in \mathbb{Z}$. Therefore the frequency switches from being discrete to continuum as α changes with r .

2.2.2 Gödel's universe:

Gödel's universe is another famous example that admit closed timelike curves [25]. Gödel's universe is an exact solution of Einstein Field equations. However it is not a spacetime in the sense of the definition because it is not everywhere Lorentzian: Gödel's universe admits two timelike directions at some part of the universe. Closed timelike curves exist with the appearance of this second timelike direction.

The metric of Gödel's universe is [3]:

$$g_{ij}dx^i dx^j = -dt^2 + dx^2 - \frac{1}{2}e^{2\sqrt{2}\Omega x}dy^2 + dz^2 - 2e^{\sqrt{2}\Omega x}dtdy \quad (2.2.22)$$

where Ω is a constant.

After a coordinate transformation to cylindrical coordinates, in new coordinates the metric takes the form:

$$g_{ij}dx^i dx^j = 2\Omega^{-2}(-dt'^2 + dr^2 - (\sinh^4 r - \sinh^2 r)d\theta^2 + 2\sqrt{2}\sinh^2 r d\theta dt' + dz^2) \quad (2.2.23)$$

This behaviour of the null cones in this metric is similar to that of 2.2.18 and closed timelike curves appears when $r > \log(1 + \sqrt{2})$.

The solution of scalar wave equation in Gödel's universe is given in [26]. In agreement with the above results, the frequency can take discrete values in Gödel's universe:

$$\omega = (1 + 2n)\Omega + \sqrt{(2n^2 + 2n + 1)\Omega + k_3^2}, \quad n \in \mathbb{Z} \quad (2.2.24)$$

where k_3 is the wavenumber in z direction. The solution for a more general class of universes with papapetrou metric has similar properties [27].

In all these class of spacetimes where closed timelike curves are admissible throughout the manifold, the common property is frequency selection. Frequency is not continuum and only a discrete set of frequencies can exist in these universes.

CHAPTER 3

SCALAR WAVES IN A WORMHOLE SPACETIME

Wormholes are another very important class of spacetimes that may admit closed timelike curves (CTC). In wormholes, however closed timelike and null curves are restricted to pass around the throat of the wormhole and in general there does not exist a CTC passing from an arbitrary point of wormhole.

3.1 Flat wormhole

Given a Riemannian manifold M , a solution $F : M \times \mathbb{R} \rightarrow \mathbb{C}$ of the scalar wave equation

$$\Delta F = \frac{\partial^2 F}{\partial t^2}$$

is said to be a *monochromatic solution* with angular frequency $\omega \in \mathbb{R} - \{0\}$ if it is of the form $F(m, t) = \Psi(m)e^{i\omega t}$ for some $\Psi : M \rightarrow \mathbb{C}$. Clearly Ψ is a solution of the Helmholtz equation

$$\Delta \Psi + \omega^2 \Psi = 0. \tag{3.1.1}$$

On a general Lorentzian spacetime the concept of monochromatic solution makes sense provided the spacetime has an almost product structure that singles out the time direction locally.

A simple example of a wormhole topology is the flat wormhole described in [19]. This 3+1 dimensional flat wormhole spacetime is constructed as follows: Let

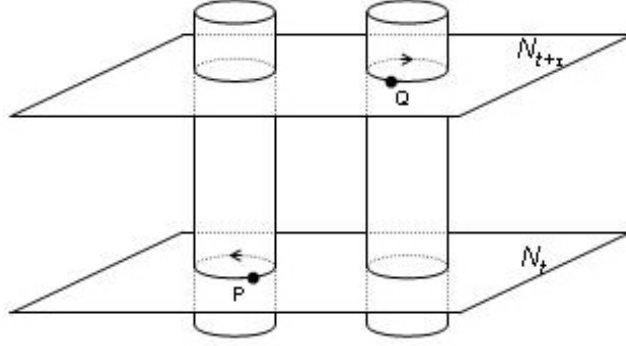


Figure 3.1: 2+1 dimensional flat wormhole. P is identified with Q . Arrows indicate the direction of the identification.

$a, d, \tau \in \mathbb{R}$ with $d > 2a > 0$. Consider

$$N = \mathbb{R}^3 - (\Delta_+ \cup \Delta_-),$$

$$\hat{M} = N \times \mathbb{R},$$

where Δ_+, Δ_- are open balls of radius $a > 0$ and respective centers $(0, 0, d/2), (0, 0, -d/2)$ in \mathbb{R}^3 . The boundaries of Δ_+ and Δ_- are designated as Σ_+ and Σ_- respectively. The *wormhole spacetime* M of width d , radius a , and lag τ is the Semi-Riemannian manifold obtained as the quotient space of \hat{M} by identifying events P, Q on $\Sigma_+ \times \mathbb{R}, \Sigma_- \times \mathbb{R}$ respectively if P is the reflection of Q in the xyt -hyperplane after a translation by τ along the t -axis, the Semi-Riemannian metric being naturally inherited from the ordinary Minkowski metric on \mathbb{R}^4 . M is clearly a flat Lorentzian spacetime. To be precise:

$$\Sigma_+ = \{(x, y, z) \in \mathbb{R}^3 | x^2 + y^2 + (z - d/2)^2 = a^2\},$$

$$\Sigma_- = \{(x, y, z) \in \mathbb{R}^3 | x^2 + y^2 + (z + d/2)^2 = a^2\}.$$

For $(x, y, z) \in \Sigma_+$, P and Q are identified where

$$P = (x, y, z, t),$$

$$Q = (x, y, -z, t + \tau).$$

In 2+1 dimensions the manifold is defined in the same way except that:

$$N = (\mathbb{R}^2 - (\Delta_+ \cup \Delta_-)),$$

Δ_+, Δ_- are open disks of radius $a > 0$ with respective centers $(d/2, 0), (-d/2, 0)$ in \mathbb{R}^2 and P is the reflection of Q in the yt - plane after a translation by τ along the t -axis.

The geometry for 2+1 dimensions is shown in fig. 3.1.

Two wormhole conditions arise from this identification map defining the topology. These conditions will function as boundary conditions imposed on the general solution of Helmholtz equation in a flat spacetime.

The two wormhole conditions will be denoted as C-1 and C-2. C-1 is

$$F(P) = F(Q),$$

and C-2 is

$$\hat{n}_P \cdot \nabla F(P) = -\hat{n}_Q \cdot \nabla F(Q).$$

where \hat{n}_Q is the unit outward normal to Σ_- at Q and \hat{n}_P is the unit outward normal to Σ_+ at P . In terms of Ψ , C-1 and C-2 are:

$$\Psi(\omega, p) = e^{i\omega\tau} \Psi(\omega, q),$$

$$\hat{n}_P \cdot \nabla \Psi(\omega, p) = -e^{i\omega\tau} \hat{n}_Q \cdot \nabla \Psi(\omega, q),$$

where p and q are the projections of P and Q on N respectively.

The solution will be expressed in three components: An everywhere regular part of the wave, Ψ_0 , which may be considered as originating from the sources at past null infinity (or alternatively as the incident wave if the problem is considered as a

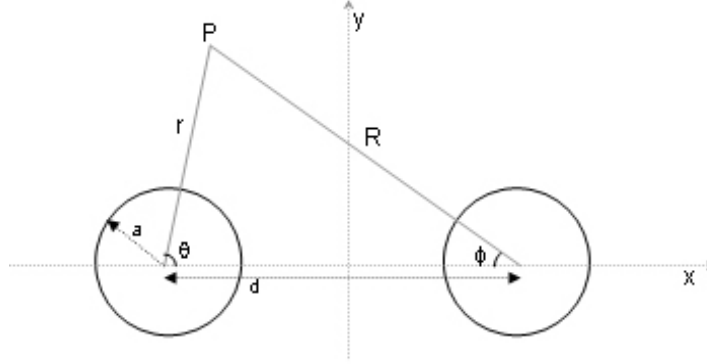


Figure 3.2: Coordinates used for 2+1 dimensions.

scattering problem), and two outgoing waves originating from each wormhole mouth (or scattered waves from each mouth), Ψ_1 and Ψ_2 . Obviously $\Psi = \Psi_0 + \Psi_1 + \Psi_2$.

There are two wormhole conditions that enable one to determine two of Ψ_0 , Ψ_1 and Ψ_2 . The problem will be handled like a scattering problem and the scattered waves Ψ_1 and Ψ_2 . will be solved given the incident wave Ψ_0 .

3.2 2+1 Dimensions:

In 2+1 dimensions, solution of Helmholtz equation in cylindrical coordinates yields Bessel (or Hankel) functions. Being everywhere regular, Ψ_0 is expressed in terms of $J_n(r)$, while Ψ_1 and Ψ_2 represent outgoing waves radiating from the wormhole mouths Δ_- and Δ_+ , respectively. Outgoing waves are expressed by Hankel functions of the first kind, $H_n^{(1)}(r)$. Referring to fig. 3.2, Ψ_1 has its natural coordinates (r, θ) centered at $(-d/2, 0)$, and Ψ_2 has its natural coordinates (R, ϕ) centered at $(d/2, 0)$. The coordinate variables, θ and ϕ are chosen in this way to make use of the mirror symmetry of the geometry of the wormhole with respect to y axis. Since Ψ_0 , Ψ_1 and Ψ_2 are valid in exterior domain, they are expressed in terms of integer order Bessel (Hankel) functions only. Therefore the expansion of Ψ_0 , Ψ_1 and Ψ_2 in terms of Bessel (Hankel) functions are:

$$\begin{aligned}
\Psi_0 &= \sum_{n=-\infty}^{\infty} A_n J_n(\omega r) e^{in\theta}, \\
\Psi_1 &= \sum_{n=-\infty}^{\infty} B_n H_n^{(1)}(\omega r) \cdot e^{in\theta}, \\
\Psi_2 &= \sum_{n=-\infty}^{\infty} C_n H_n^{(1)}(\omega R) \cdot e^{in\phi}.
\end{aligned}$$

B_n and C_n will be found given the coefficients of the incident wave A_n . The two wormhole conditions supply the two equations to determine the unknown coefficients B_n and C_n .

The wormhole conditions C-1 and C-2 are:

$$\begin{aligned}
\Psi|_{R=a, \phi=\theta} &= e^{i\omega\tau} \Psi|_{r=a} \quad -\pi < \theta \leq \pi, \\
\frac{\partial}{\partial R} \Psi|_{R=a, \phi=\theta} &= -e^{i\omega\tau} \frac{\partial}{\partial r} \Psi|_{r=a} \quad -\pi < \theta \leq \pi.
\end{aligned}$$

To compute Ψ at $R = a$ and $r = a$ it is necessary to write down Ψ_0, Ψ_1 in (R, ϕ) coordinates and Ψ_2 in (r, θ) coordinates. The addition theorem for cylindrical harmonics is used for expressing a cylindrical wave in terms of cylindrical waves of a translated origin [24]. It should be noted that, unlike the everywhere regular Bessel functions $J_n(\omega r)$, there are two different versions of the addition theorems of Hankel functions. For $\vec{r} = \vec{d} + \vec{R}$, addition theorems yield

$$H_n^{(1)}(\omega R)e^{in(\pi-\phi)} = \begin{cases} \sum_{k=-\infty}^{\infty} J_k(\omega d) H_{n+k}^{(1)}(\omega r) e^{i(n+k)\theta} & \text{if } r > d \\ \sum_{k=-\infty}^{\infty} H_k^{(1)}(\omega d) J_{n+k}(\omega r) e^{i(n+k)\theta} & \text{if } r < d \end{cases}, \quad (3.2.2)$$

$$H_n^{(1)}(\omega r)e^{in(\theta-\pi)} = \begin{cases} \sum_{k=-\infty}^{\infty} J_k(\omega d) H_{n+k}^{(1)}(\omega R) e^{-i(n+k)\phi} & \text{if } R > d \\ \sum_{k=-\infty}^{\infty} H_k^{(1)}(\omega d) J_{n+k}(\omega R) e^{-i(n+k)\phi} & \text{if } R < d \end{cases}, \quad (3.2.3)$$

$$J_n(\omega r)e^{in(\theta-\pi)} = \sum_{k=-\infty}^{\infty} J_k(\omega d) J_{n+k}(\omega R) e^{-i(n+k)\phi}. \quad (3.2.4)$$

Wormhole conditions require the expression at $r = a$ and $R = a$. Since $a < d$, $r < d$ versions of (3.2.2) and (3.2.3) should be used.

Accordingly, the wave functions are expressed as a sum of Bessel functions at translated origin as

$$\begin{aligned} \sum_{n=-\infty}^{\infty} A_n J_n(\omega r) e^{in\theta} &= \sum_{n=-\infty}^{\infty} \bar{A}_n \cdot J_n(\omega R) e^{in\phi}, \\ \sum_{n=-\infty}^{\infty} B_n H_n^{(1)}(\omega r) e^{in\theta} &= \sum_{n=-\infty}^{\infty} \bar{B}_n \cdot J_n(\omega R) \cdot e^{in\phi}, \\ \sum_{n=-\infty}^{\infty} C_n H_n^{(1)}(\omega R) e^{in\phi} &= \sum_{n=-\infty}^{\infty} \bar{C}_n \cdot J_n(\omega r) \cdot e^{in\theta}. \end{aligned}$$

The expressions for \bar{A}_n , \bar{B}_n and \bar{C}_n are found using (3.2.2), (3.2.3) and (3.2.4). For \bar{A}_n :

$$\Psi_0 = \sum_{n=-\infty}^{\infty} A_n J_n(\omega r) e^{in\theta} = \sum_{n=-\infty}^{\infty} A_n (-1)^n \sum_{k=-\infty}^{\infty} J_k(\omega d) J_{n+k}(\omega R) e^{-i(n+k)\phi} \quad (3.2.5)$$

Renaming the index $-(n+k) = n$ on the right hand side and using $(-1)^n J_n(x) = J_{-n}(x)$:

$$\sum_{n=-\infty}^{\infty} A_n J_n(\omega r) e^{in\theta} = \sum_{n=-\infty}^{\infty} \sum_{k=-\infty}^{\infty} A_{-n-k} (-1)^{-n-k} J_k(\omega d) J_{-n}(\omega R) e^{in\phi} \quad (3.2.6)$$

$$= \sum_{n=-\infty}^{\infty} \left(\sum_{k=-\infty}^{\infty} A_{-n-k} J_{-k}(\omega d) \right) J_n(\omega R) e^{in\phi} \quad (3.2.7)$$

$$= \sum_{n=-\infty}^{\infty} \left(\sum_{k=-\infty}^{\infty} A_{k-n} J_k(\omega d) \right) J_n(\omega R) e^{in\phi} \quad (3.2.8)$$

Similarly for \bar{B}_n :

$$\begin{aligned} \Psi_1 &= \sum_{n=-\infty}^{\infty} B_n H_n^{(1)}(\omega r) \cdot e^{in\theta} = \sum_{n=-\infty}^{\infty} B_n (-1)^n \sum_{k=-\infty}^{\infty} H_k^{(1)}(\omega d) J_{n+k}(\omega R) e^{-i(n+k)\phi} \\ &= \sum_{n=-\infty}^{\infty} \sum_{k=-\infty}^{\infty} B_{-n-k} (-1)^{-n-k} H_k^{(1)}(\omega d) J_{-n}(\omega R) e^{in\phi} \\ &= \sum_{n=-\infty}^{\infty} \left(\sum_{k=-\infty}^{\infty} B_{-n-k} H_{-k}^{(1)}(\omega d) \right) J_n(\omega R) e^{in\phi} \\ &= \sum_{n=-\infty}^{\infty} \left(\sum_{k=-\infty}^{\infty} B_{k-n} H_k^{(1)}(\omega d) \right) J_n(\omega R) e^{in\phi} \quad (3.2.9) \end{aligned}$$

The translation direction for \bar{C}_n is reverse and translation formula is slightly different. However choosing the ϕ mirror image of θ , results in the same formula for \bar{C}_n either:

$$\Psi_2 = \sum_{n=-\infty}^{\infty} C_n H_n^{(1)}(\omega R) \cdot e^{in\phi} = \sum_{n=-\infty}^{\infty} C_n \sum_{k=-\infty}^{\infty} H_k^{(1)}(\omega d) J_{-n+k}(\omega r) e^{i(-n+k)\theta} \quad (3.2.10)$$

Renaming the index $-n + k = n$ on the right hand side:

$$\Psi_2 = \sum_{n=-\infty}^{\infty} \left(\sum_{k=-\infty}^{\infty} C_{k-n} H_k^{(1)}(\omega d) \right) J_n(\omega r) e^{in\theta} \quad (3.2.11)$$

Therefore the formulas for \bar{A}_n , \bar{B}_n and \bar{C}_n are:

$$\bar{A}_n = \sum_{k=-\infty}^{\infty} A_{k-n} J_k(\omega d), \quad (3.2.12)$$

$$\bar{B}_n = \sum_{k=-\infty}^{\infty} B_{k-n} H_k^{(1)}(\omega d), \quad (3.2.13)$$

$$\bar{C}_n = \sum_{k=-\infty}^{\infty} C_{k-n} H_k^{(1)}(\omega d). \quad (3.2.14)$$

Having obtained the expression of the wave in the coordinates centered at each mouth, application of wormhole conditions give necessary equations for the unknown coefficients B_n and C_n .

C-1 leads to

$$\begin{aligned} \sum_{n=-\infty}^{\infty} (A_n \cdot J_n(\omega a) + B_n \cdot H_n^{(1)}(\omega a) + \bar{C}_n J_n(\omega a)) e^{in\theta} \\ = e^{i\omega\tau} \sum_{n=-\infty}^{\infty} (\bar{A}_n J_n(\omega a) + \bar{B}_n J_n(\omega a) + C_n \cdot H_n^{(1)}(\omega a)) e^{in\theta}, \end{aligned}$$

$$B_n - e^{i\omega\tau} C_n = -\frac{J_n(\omega a)}{H_n^{(1)}(\omega a)} (A_n - e^{i\omega\tau} \bar{A}_n + \bar{C}_n - e^{i\omega\tau} \bar{B}_n), \quad (3.2.15)$$

and C-2 leads to

$$\begin{aligned} \sum_{n=-\infty}^{\infty} \left(A_n \cdot \frac{\partial}{\partial r} J_n(\omega r)|_{r=a} + B_n \cdot \frac{\partial}{\partial r} H_n^{(1)}(\omega r)|_{r=a} + \bar{C}_n \frac{\partial}{\partial r} J_n(\omega r)|_{r=a} \right) e^{in\theta} \\ = -e^{i\omega\tau} \sum_{n=-\infty}^{\infty} \left(\bar{A}_n \frac{\partial}{\partial r} J_n(\omega r)|_{r=a} + \bar{B}_n \frac{\partial}{\partial r} J_n(\omega r)|_{r=a} + C_n \frac{\partial}{\partial r} H_n^{(1)}(\omega r)|_{r=a} \right) e^{in\theta}, \end{aligned}$$

$$B_n + e^{i\omega\tau} C_n = -\frac{\frac{\partial}{\partial r} J_n(\omega r)|_{r=a}}{\frac{\partial}{\partial r} H_n^{(1)}(\omega r)|_{r=a}} (A_n + e^{i\omega\tau} \bar{A}_n + \bar{C}_n + e^{i\omega\tau} \bar{B}_n). \quad (3.2.16)$$

Solving (3.2.15) and (3.2.16) for B_n and C_n , one finds

$$B_n = -\gamma_n^+(\omega a) \bar{C}_n + e^{i\omega\tau} \gamma_n^-(\omega a) \bar{B}_n - \gamma_n^+(\omega a) A_n + e^{i\omega\tau} \gamma_n^-(\omega a) \bar{A}_n, \quad (3.2.17)$$

$$C_n = -\gamma_n^+(\omega a) \bar{B}_n + e^{-i\omega\tau} \gamma_n^-(\omega a) \bar{C}_n - \gamma_n^+(\omega a) \bar{A}_n + e^{-i\omega\tau} \gamma_n^-(\omega a) A_n, \quad (3.2.18)$$

where

$$\gamma_n^+(\omega a) \triangleq \frac{1}{2} \left(\frac{J_n(\omega a)}{H_n^{(1)}(\omega a)} + \frac{\frac{\partial}{\partial r} J_n(\omega r)|_{r=a}}{\frac{\partial}{\partial r} H_n^{(1)}(\omega r)|_{r=a}} \right),$$

$$\gamma_n^-(\omega a) \triangleq \frac{1}{2} \left(\frac{J_n(\omega a)}{H_n^{(1)}(\omega a)} - \frac{\frac{\partial}{\partial r} J_n(\omega r)|_{r=a}}{\frac{\partial}{\partial r} H_n^{(1)}(\omega r)|_{r=a}} \right).$$

For the sake of simplicity the known parts of (3.2.17) and (3.2.18) will be denoted by E_n and F_n respectively.

$$E_n = -\gamma_n^+(\omega a) A_n + e^{i\omega\tau} \gamma_n^-(\omega a) \bar{A}_n, \quad (3.2.19)$$

$$F_n = -\gamma_n^+(\omega a) \bar{A}_n + e^{-i\omega\tau} \gamma_n^-(\omega a) A_n. \quad (3.2.20)$$

This pair of equations (3.2.17) and (3.2.18) are not solvable explicitly; however it is possible to solve them for the limiting cases $a \ll d$ and $a \ll 1$.

3.2.1 Solutions for $a \ll d$ and $a \ll 1$:

The difficulty in solving (3.2.17) and (3.2.18) arises from the convolution sum present in the expressions of \bar{B}_n and \bar{C}_n . However this term can be evaluated for special forms of $H_n^{(1)}(\omega d)$, namely when it is in complex exponential $e^{-in\alpha}$ form. When $|n| \ll \omega d$, asymptotically $H_n^{(1)}(\omega d)$ becomes $e^{-in\pi/2}$ as a function of n . $\gamma_n^+(\omega a)$ and $\gamma_n^-(\omega a)$ are almost zero for $|n| \gtrsim 2\omega a$, and so are B_n and C_n . Thus when $a \ll d$, the only terms that contribute to $\gamma_n^\pm(\omega a)\bar{B}_n$ ($\gamma_n^\pm(\omega a)\bar{C}_n$) are those satisfy $|n| \lesssim 2\omega a \ll \omega d$. The $a \ll d$ case is of practical importance in physics. In a wormhole universe, this corresponds to the case that the wormhole is connecting regions of the universe that are spatially far from each other compared to the radius of the wormhole.

This approximation is not valid for the high frequency limit in general.

When $a \ll 1$, $\gamma_n^\pm(\omega a)$ tends to zero unless $n \neq 0$, regardless of d . Accordingly, so are B_n and C_n .

These two cases in which approximate solutions are possible, $a \ll d$ and $a \ll 1$, are examined below.

$a \ll d$

For large ωd , asymptotic formula for $H_n^{(1)}(\omega d)$ is

$$H_n^{(1)}(\omega d) = z(\omega d)e^{-in\pi/2} \quad (3.2.21)$$

$$\times \left(1 + i\frac{4n^2 - 1}{1!(8\omega d)} + i^2\frac{(4n^2 - 1)(4n^2 - 9)}{2!(8\omega d)^2} + i^3\frac{(4n^2 - 1)(4n^2 - 9)(4n^2 - 25)}{3!(8\omega d)^3} + \dots\right),$$

$$z(\omega d) \triangleq \sqrt{\frac{2}{\pi\omega d}} e^{i(\omega d - (\pi/4))}.$$

For $n^2 \ll \omega d$, the infinite sum inside the brackets can be approximated to 1 :

$$H_n^{(1)}(\omega d) \approx z(\omega d)e^{-in\pi/2}$$

This form of $H_n^{(1)}(\omega d)$ allows one to evaluate the sum \bar{B}_n :

$$\begin{aligned}
\sum_{k=-\infty}^{\infty} B_{(k-n)} H_k^{(1)}(\omega d) &= \sum_{m=-\infty}^{\infty} B_m H_{n+m}^{(1)}(\omega d) \approx z(\omega d) \left(\sum_{m=-\infty}^{\infty} B_m e^{-im\pi/2} \right) e^{-in\pi/2} \\
&= z(\omega d) \hat{B}(\pi/2) e^{-in\pi/2}
\end{aligned}$$

where hat denotes the Fourier sum:

$$\hat{X}(\alpha) \triangleq \sum_{m=-\infty}^{\infty} X_m e^{-im\alpha}.$$

Substituting into (3.2.17) and (3.2.18)

$$B_n = z(\omega d) [-\hat{C}(\pi/2) \gamma_n^+ + e^{i\omega\tau} \hat{B}(\pi/2) \gamma_n^-] e^{-in\pi/2} + E_n, \quad (3.2.22)$$

$$C_n = z(\omega d) [-\hat{B}(\pi/2) \gamma_n^+ + e^{-i\omega\tau} \hat{C}(\pi/2) \gamma_n^-] e^{-in\pi/2} + F_n. \quad (3.2.23)$$

The right hand sides of (3.2.22) and (3.2.23) involves $\hat{C}(\pi/2)$ and $\hat{B}(\pi/2)$ which are unknown yet. Multiplying each side by $e^{-in\pi/2}$ and sum over n 's gives a pair of equations for $\hat{C}(\pi/2)$ and $\hat{B}(\pi/2)$:

$$\begin{bmatrix} \hat{B}(\pi/2) \\ \hat{C}(\pi/2) \end{bmatrix} = \begin{bmatrix} 1 - z(\omega d) e^{i\omega\tau} \tilde{\gamma}^-(\pi) & z(\omega d) \tilde{\gamma}^+(\pi) \\ z(\omega d) \tilde{\gamma}^+(\pi) & 1 - z(\omega d) e^{-i\omega\tau} \tilde{\gamma}^-(\pi) \end{bmatrix}^{-1} \begin{bmatrix} \hat{E}(\pi/2) \\ \hat{F}(\pi/2) \end{bmatrix} \quad (3.2.24)$$

The numerical results comparing the solutions obtained by these formulae and by the multiple scattering method is presented in the appendix.

To have a better approximation, the second term $i \frac{4n^2 - 1}{1!(8\omega d)}$ in the infinite sum of in (3.2.21) can be included:

$$H_n^{(1)}(\omega d) \approx \sqrt{\frac{2}{\pi\omega d}} e^{i(\omega d - (\pi/4))} e^{-in\pi/2} \left(1 + i \frac{4n^2 - 1}{1!(8z)} \right)$$

In this case, the expression for $H_n^{(1)}(\omega d)$ involves $n^2 e^{-in\pi/2}$. This form of $H_n^{(1)}(\omega d)$ still enables one to evaluate \bar{B}_n and \bar{C}_n , explicitly. This time there arise 6 unknowns

and (3.2.24) is replaced by a 6x6 matrix equation. In this way it is possible to have better approximations by taking more terms into account in (3.2.21). The number of the linear equations is $4k - 2$ when the first k term is taken into account in (3.2.21).

$a \ll 1$:

At $\omega a = 0$, the Bessel function $J_n(\omega a)$ is a discrete delta function with respect to variable n , and its derivative is zero for all n :

$$J_n(0) = \begin{cases} 1 & \text{if } n = 0 \\ 0 & \text{otherwise} \end{cases} ; \quad \frac{\partial}{\partial r} J_n(\omega r)|_{r=0} = 0 \text{ for all } n. \quad (3.2.25)$$

Therefore, in the limit a goes to zero, $\gamma_n^+(\omega a)$ and $\gamma_n^-(\omega a)$ become discrete delta functions:

$$\gamma_n^+(\omega a) \approx \gamma_n^-(\omega a) \approx \frac{J_0(\omega a)}{H_0^{(1)}(\omega a)} \delta_n,$$

where [28],

$$\frac{J_0(\omega a)}{H_0^{(1)}(\omega a)} \triangleq \gamma_0 = \frac{1}{1 + \frac{2i}{\pi}(\ln(\frac{\omega a}{2}) + 0.5772)}. \quad (3.2.26)$$

The $\gamma_n^\pm(\omega a)$ factors standing in front of each term on the right hand sides of (3.2.17) and (3.2.18) make B_n and C_n delta functions as well.

$$B_n = B_0 \delta_n,$$

$$C_n = C_0 \delta_n;$$

so that,

$$\Psi_1 = B_0 \cdot H_0^{(1)}(\omega r),$$

$$\Psi_2 = C_0 \cdot H_0^{(1)}(\omega R).$$

B_0 and C_0 are found by substitution to (3.2.17) and (3.2.18):

$$\begin{aligned}\gamma_n^\pm(\omega a)\bar{B}_n &\approx (\gamma_0\delta_n)(B_0H_n^{(1)}(\omega d)) = \gamma_0B_0H_0^{(1)}(\omega d)\delta_n, \\ \gamma_n^\pm(\omega a)\bar{C}_n &\approx \gamma_0C_0H_0(\omega d)\delta_n,\end{aligned}$$

$$\begin{bmatrix} B_0 \\ C_0 \end{bmatrix} = \begin{bmatrix} 1 - \gamma_0H_0(\omega d)e^{i\omega\tau} & \gamma_0H_0(\omega d) \\ \gamma_0H_0(\omega d) & 1 - \gamma_0H_0(\omega d)e^{-i\omega\tau} \end{bmatrix}^{-1} \begin{bmatrix} E_0 \\ F_0 \end{bmatrix},$$

where

$$\begin{aligned}E_0 &= \gamma_0(-A_0 + e^{i\omega\tau} \sum_{m=-\infty}^{\infty} A_m J_m(\omega d)), \\ F_0 &= \gamma_0(- \sum_{m=-\infty}^{\infty} A_m J_m(\omega d) + e^{-i\omega\tau} A_0).\end{aligned}$$

3.2.2 Multiple scattering

An alternative approach is the use of multiple scattering [20],[29]. In the multiple scattering method, the scattered waves are decomposed into lower order scattered waves from each mouth. Initially each wormhole mouth is considered to be excited by only the incident wave and first order scattering coefficients are found by imposing wormhole conditions. Then each wormhole is considered to be excited by only the first order scattered wave from the other mouth and the second order scattering coefficient are found imposing wormhole conditions. k^{th} order scattering coefficients are found by continuing the same procedure. The scattered wave from each mouth is the sum of these k^{th} order scattering coefficients.

$$\Psi_1 = \sum_{k=1}^{\infty} \Psi_1^k$$

where

$$\Psi_1^k = \sum_{n=-\infty}^{\infty} B_n^k H_n^{(1)}(\omega r) \cdot e^{in\theta} \text{ and } B_n = \sum_{k=1}^{\infty} B_n^k.$$

Similarly,

$$\begin{aligned} \Psi_2 &= \sum_{k=1}^{\infty} \Psi_2^k, \\ \Psi_2^k &= \sum_{n=-\infty}^{\infty} C_n^k H_n^{(1)}(\omega R) \cdot e^{in\phi}. \end{aligned}$$

Wormhole conditions for the first order scattering coefficients are:

$$(\Psi_0 + \Psi_1^1)_{r=a} = e^{i\omega\tau} (\Psi_0 + \Psi_2^1)_{R=a, \phi=\theta}, \quad (3.2.27)$$

$$\frac{\partial}{\partial r} (\Psi_0 + \Psi_1^1)|_{r=a} = -e^{i\omega\tau} \frac{\partial}{\partial R} (\Psi_0 + \Psi_2^1)|_{R=a, \phi=\theta}. \quad (3.2.28)$$

Similarly for the $(k+1)^{th}$ order coefficients:

$$\begin{aligned} (\Psi_1^{k+1} + \Psi_2^k)_{r=a} &= e^{i\omega\tau} (\Psi_1^k + \Psi_2^{k+1})|_{R=a, \phi=\theta}, \\ \frac{\partial}{\partial r} (\Psi_1^{k+1} + \Psi_2^k)|_{r=a} &= -e^{i\omega\tau} \frac{\partial}{\partial R} (\Psi_1^k + \Psi_2^{k+1})|_{R=a, \phi=\theta}. \end{aligned}$$

It is easy to see that when 1^{st} and k^{th} order scattered waves satisfy wormhole conditions, total scattered wave satisfies as well.

$$\begin{aligned} \Psi|_{r=a} &= (\Psi_0 + \Psi_1 + \Psi_2)|_{r=a} = (\Psi_0 + \Psi_1^1 + \sum_{k=1}^{\infty} (\Psi_1^{k+1} + \Psi_2^k))|_{r=a} \\ &= e^{i\omega\tau} (\Psi_0 + \Psi_2^1)|_{R=a, \phi=\theta} + e^{i\omega\tau} \sum_{k=1}^{\infty} (\Psi_1^k + \Psi_2^{k+1})|_{R=a, \phi=\theta} = e^{i\omega\tau} (\Psi_0 + \Psi_1 + \Psi_2)|_{R=a, \phi=\theta}. \end{aligned}$$

Imposing wormhole conditions to (3.2.27) and (3.2.28), first order scattering

coefficients are obtained.

C-1 yields:

$$\sum_{n=-\infty}^{\infty} A_n \cdot J_n(\omega a) e^{in\theta} + B_n^1 \cdot H_n^{(1)}(\omega a) \cdot e^{in\theta} = e^{i\omega\tau} \left(\sum_{n=-\infty}^{\infty} \bar{A}_n J_n(\omega a) e^{in\theta} + \sum_{n=-\infty}^{\infty} C_n^1 H_n^{(1)}(\omega a) \cdot e^{in\theta} \right),$$

$$B_n^1 - e^{i\omega\tau} C_n^1 = -\frac{J_n(\omega a)}{H_n^{(1)}(\omega a)} (A_n - e^{i\omega\tau} \bar{A}_n).$$

C-2 yields:

$$B_n^1 + e^{i\omega\tau} C_n^1 = -\frac{\frac{\partial}{\partial r} J_n(\omega r)|_{r=a}}{\frac{\partial}{\partial r} H_n^{(1)}(\omega r)|_{r=a}} (A_n + e^{i\omega\tau} \bar{A}_n).$$

Solving for B_n^1 and C_n^1 :

$$B_n^1 = -\gamma_n^+(\omega a) A_n + e^{i\omega\tau} \gamma_n^-(\omega a) \bar{A}_n, \quad (3.2.29)$$

$$C_n^1 = -\gamma_n^+(\omega a) \bar{A}_n + e^{-i\omega\tau} \gamma_n^-(\omega a) A_n. \quad (3.2.30)$$

Note that B_n^1 and C_n^1 are equal to the known parts of (3.2.17) and (3.2.18), E_n and F_n , respectively.

k^{th} order scattering coefficients are obtained similarly as:

$$B_n^{k+1} = -\gamma_n^+(\omega a) \bar{C}_n^k + e^{i\omega\tau} \gamma_n^-(\omega a) \bar{B}_n^k, \quad (3.2.31)$$

$$C_n^{k+1} = -\gamma_n^+(\omega a) \bar{B}_n^k + e^{-i\omega\tau} \gamma_n^-(\omega a) \bar{C}_n^k. \quad (3.2.32)$$

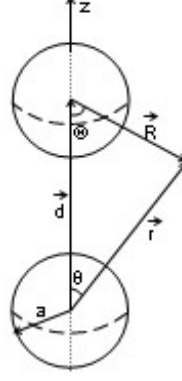


Figure 3.3: Coordinates used for 3+1 dimensions.

3.3 3+1 Dimensions

In 3+1 dimensions, the solutions of wave equation in spherical coordinates, i.e. spherical wave functions, involve spherical Bessel functions and spherical harmonics [30]. In agreement with the 2+1 dimensional case, Ψ_0 is expressed in terms of usual spherical Bessel functions, while Ψ_1 and Ψ_2 are expressed in terms of spherical Hankel functions. Referring to fig.3.3,

$$\Psi_0 = \sum_{l=-\infty}^{\infty} \sum_{m=-l}^l A_{lm} \cdot j_l(\omega r) Y_{lm}(\theta, \varphi), \quad (3.3.33)$$

$$\Psi_1 = \sum_{l=-\infty}^{\infty} \sum_{k=-l}^l B_{lm} \cdot h_l^{(1)}(\omega r) Y_{lm}(\theta, \varphi), \quad (3.3.34)$$

$$\Psi_2 = \sum_{l=-\infty}^{\infty} \sum_{m=-l}^l C_{lm} \cdot h_l^{(1)}(\omega R) Y_{lm}(\Theta, \varphi), \quad (3.3.35)$$

and the wormhole conditions are,

$$\begin{aligned}\Psi|_{r=a} &= e^{i\omega\tau}\Psi|_{R=a,\Theta=\theta}; & 0 \leq \theta \leq \pi, \quad -\pi < \varphi \leq \pi, \\ \frac{\partial}{\partial r}\Psi|_{r=a} &= -e^{i\omega\tau}\frac{\partial}{\partial R}\Psi|_{R=a,\Theta=\theta}; & 0 \leq \theta \leq \pi, \quad -\pi < \varphi \leq \pi.\end{aligned}$$

The addition theorems for the spherical wave functions, for $\vec{r} = \vec{d} + \vec{R}$ are [31],[32]:

$$j_l(\omega r)Y_{lm}(\theta, \varphi) = \sum_{l'm'} \alpha_{l'm'}^{lm+}(\vec{d}) j_{l'}(\omega R)Y_{l'm'}(\pi - \Theta, \varphi), \quad (3.3.36)$$

$$h_l^{(1)}(\omega r)Y_{lm}(\theta, \varphi) = \sum_{l'm'} \alpha_{l'm'}^{lm}(\vec{d}) j_{l'}(\omega R)Y_{l'm'}(\pi - \Theta, \varphi) \quad \text{for } R < d, \quad (3.3.37)$$

$$h_l^{(1)}(\omega R)Y_{lm}(\pi - \Theta, \varphi) = \sum_{l'm'} \alpha_{l'm'}^{lm}(-\vec{d}) j_{l'}(\omega r)Y_{l'm'}(\theta, \varphi) \quad \text{for } r < d, \quad (3.3.38)$$

where

$$\begin{aligned}\alpha_{l'm'}^{lm+}(\vec{x}) &\triangleq \sum_{\lambda\mu} c(lm|l'm'|\lambda\mu) j_\lambda(\omega|x|)Y_{\lambda\mu}(\hat{x}), \\ \alpha_{l'm'}^{lm}(\vec{x}) &\triangleq \sum_{\lambda\mu} c(lm|l'm'|\lambda\mu) h_\lambda^{(1)}(\omega|x|)Y_{\lambda\mu}(\hat{x}).\end{aligned} \quad (3.3.39)$$

The coefficients $c(lm|l'm'|\lambda\mu)$ in terms of 3-j symbols are:

$$c(lm|l'm'|\lambda\mu) = i^{l+\lambda-1}(-1)^m [4\pi(2l+1)(2l'+1)(2\lambda+1)]^{1/2} \begin{pmatrix} l & l' & \lambda \\ 0 & 0 & 0 \end{pmatrix} \begin{pmatrix} l & l' & \lambda \\ m & -m' & \mu \end{pmatrix} \quad (3.3.40)$$

The expansion (3.3.37) and (3.3.38) are valid for $R < d$ and $r < d$, respectively and they cover region where the wormhole conditions are imposed: $R = a$ and $r = a$, ($a < d$).

Using (3.3.36), (3.3.37) and (3.3.38), Ψ_0, Ψ_1 and Ψ_2 are expressed as a sum of wave functions at translated origin as:

$$\begin{aligned}
\sum_{lm} A_{lm} \cdot j_l(\omega r) Y_{lm}(\theta, \varphi) &= \sum_{lm} \bar{A}_{lm} j_l(\omega R) Y_{lm}(\Phi, \varphi), \\
\sum_{lm} B_{lm} \cdot h_l^{(1)}(\omega r) Y_{lm}(\theta, \varphi) &= \sum_{lm} \bar{B}_{lm} j_l(\omega r) Y_{lm}(\Phi, \varphi), \\
\sum_{lm} C_{lm} \cdot h_l^{(1)}(\omega R) Y_{lm}(\Phi, \varphi) &= \sum_{lm} \bar{C}_{lm} j_l(\omega r) Y_{lm}(\theta, \varphi).
\end{aligned}$$

where the analogues of the formulas (3.2.12), (3.2.13) and (3.2.14) are (see appendix A)

$$\bar{A}_{lm} = (-1)^{l+m} \sum_{l'm} A_{l'm} \alpha_{lm}^{l'm+}(\vec{d}), \quad (3.3.41)$$

$$\bar{B}_{lm} = (-1)^{l+m} \sum_{l'm} B_{l'm} \alpha_{lm}^{l'm}(\vec{d}), \quad (3.3.42)$$

$$\bar{C}_{lm} = (-1)^{l+m} \sum_{l'm} C_{l'm} \alpha_{lm}^{l'm}(\vec{d}). \quad (3.3.43)$$

3-j symbols are zero unless $m - m' = \mu$ [33]. Furthermore, $\vec{d} = \hat{z}d$, and $Y_{\lambda\mu}(\hat{d}) = Y_{\lambda\mu}(0, \varphi)$ is nonzero only when $\mu = 0$. Thus $m' = m$ and that's why the summation over m' drops in (3.3.41), (3.3.42) and (3.3.43)

$$\begin{aligned}
Y_{\lambda 0}(0, \varphi) &= \sqrt{\frac{2\lambda + 1}{4\pi}}, \\
\alpha_{lm}^{l'm'}(\vec{d}) &= \alpha_{lm}^{l'm}(\vec{d}) = \sum_{\lambda, \mu} c(l'm|lm|\lambda 0) h_{\lambda}^{(1)}(\omega d) \sqrt{\frac{2\lambda + 1}{4\pi}}, \\
\alpha_{lm}^{l'm'+}(\vec{d}) &= \alpha_{lm}^{l'm+}(\vec{d}) = \sum_{\lambda, \mu} c(l'm|lm|\lambda 0) j_{\lambda}(\omega d) \sqrt{\frac{2\lambda + 1}{4\pi}}.
\end{aligned}$$

Imposing the wormhole conditions and using the orthogonality of $Y_{lm}(\theta, \varphi)$ for different l, m , yields the 3+1 dimensional analogues of the equations found for 2+1 dimensions:

$$\begin{aligned}
B_{lm} - e^{i\omega\tau} C_{lm} &= -\frac{j_l(\omega a)}{h_l^{(1)}(\omega a)} (\bar{C}_{lm} - e^{i\omega\tau} \bar{B}_{lm} + A_{lm} - e^{i\omega\tau} \bar{A}_{lm}), \\
B_{lm} + e^{i\omega\tau} C_{lm} &= -\frac{\frac{\partial}{\partial r} j_l(\omega r)|_{r=a}}{\frac{\partial}{\partial r} h_l^{(1)}(\omega r)|_{r=a}} (\bar{C}_{lm} - e^{i\omega\tau} \bar{B}_{lm} + A_{lm} - e^{i\omega\tau} \bar{A}_{lm}),
\end{aligned}$$

giving

$$B_{lm} = -\gamma_l^+(\omega a) \bar{C}_{lm} + e^{i\omega\tau} \gamma_l^-(\omega a) \bar{B}_{lm} + E_{lm}, \quad (3.3.44)$$

$$C_{lm} = -\gamma_l^+(\omega a) \bar{B}_{lm} + e^{-i\omega\tau} \gamma_l^-(\omega a) \bar{C}_{lm} + F_{lm}, \quad (3.3.45)$$

where E_{lm} and F_{lm} are known functions of A_{lm} :

$$\begin{aligned}
E_{lm} &= -\gamma_l^+(\omega a) A_{lm} + e^{i\omega\tau} \gamma_l^-(\omega a) \bar{A}_{lm}, \\
F_{lm} &= -\gamma_l^+(\omega a) \bar{A}_{lm} + e^{-i\omega\tau} \gamma_l^-(\omega a) A_{lm},
\end{aligned}$$

and $\gamma_l^\pm(\omega a)$ are defined similar to 2+1 dimensional case:

$$\begin{aligned}
\gamma_l^+(\omega a) &\triangleq \frac{1}{2} \left(\frac{j_l(\omega a)}{h_l^{(1)}(\omega a)} + \frac{\frac{\partial}{\partial r} j_l(\omega r)|_{r=a}}{\frac{\partial}{\partial r} h_l^{(1)}(\omega r)|_{r=a}} \right), \\
\gamma_l^-(\omega a) &\triangleq \frac{1}{2} \left(\frac{j_l(\omega a)}{h_l^{(1)}(\omega a)} - \frac{\frac{\partial}{\partial r} j_l(\omega r)|_{r=a}}{\frac{\partial}{\partial r} h_l^{(1)}(\omega r)|_{r=a}} \right).
\end{aligned}$$

Similar to the 2+1 dimensional case, (3.3.44) and (3.3.45) can be solved for $a \ll 1$ and $a \ll d$ cases.

Solutions for $a \ll d$ and $a \ll 1$:

The asymptotic form of $h_l^{(1)}(\omega d)$ for $l \ll \omega d$ allows us to compute $\alpha_{lm}^{l'm'}(\vec{d})$. The similarity between 2+1 and 3+1 dimensional cases are remarkable. Indeed for 2+1 dimensional case, if we consider $\bar{X}_n = \sum_{k=-\infty}^{\infty} X_{k-n} H_k^{(1)}(\omega d)$ as an operator on $H_n^{(1)}(\omega d)$, the asymptotic form of $H_n^{(1)}(\omega d)$ for $n \ll \omega d$ is an eigenvalue of this operator. Similarly in the passage to the 3+1 dimensions, considering $\bar{X}_{lm} = (-1)^{l+m} \sum_{l'm'} X_{l'm'} \alpha_{lm}^{l'm'}(\vec{d})$ as an operator on $h_l^{(1)}(\omega d)$, asymptotic form of $h_l^{(1)}(\omega d)$ for $l \ll \omega d$ is an eigenfunction of \bar{X}_{lm} .

As in the 2+1 dimensional case, the presence of the $\gamma_n^{\pm}(\omega a)$ factor at each term of the right hand sides of (3.3.44) and (3.3.45), makes B_{lm} and C_{lm} vanish when $\omega a \ll l$. Thus when $a \ll d$ the asymptotic form of $h_{\lambda}^{(1)}(\omega d)$ for $l \ll \omega d$ can be used.

For $a \ll 1$, just like 2+1 dimensions, $h_l^{(1)}(\omega d)$ is zero unless $l = 0$ and (3.3.44) and (3.3.45) can be solved.

$a \ll d$:

$\gamma_l^+(\omega a)$ and $\gamma_l^-(\omega a)$ filter the terms with $l > 2\omega a$, thus when $a \ll d$ the only terms that contribute to \bar{B}_{lm} and \bar{C}_{lm} are $l \ll \omega d$. In this case $h_{\lambda}^{(1)}(\omega d)$ has the asymptotic expression:

$$h_{\lambda}^{(1)}(\omega d) \approx i^{-(\lambda+1)} \frac{e^{i\omega d}}{\omega d}$$

Then,

$$\bar{B}_{lm} \approx \sum_{l'm'} \sum_{\lambda} B_{l'm'} c(l'm|lm|\lambda 0) i^{-(\lambda+1)} \frac{e^{i\omega d}}{\omega d} \sqrt{\frac{2\lambda+1}{4\pi}}$$

Substituting

$$c(l'm|lm|\lambda 0) = i^{l'+\lambda-1} (-1)^m [4\pi(2l+1)(2l'+1)(2\lambda+1)]^{1/2} \begin{pmatrix} l & l' & \lambda \\ 0 & 0 & 0 \end{pmatrix} \begin{pmatrix} l & l' & \lambda \\ m & -m & 0 \end{pmatrix}$$

gives:

$$\bar{B}_{lm} \approx -\frac{e^{i\omega d}}{\omega d} \sum_{l'} B_{l'm} i^{l'} (-1)^m [(2l+1)(2l'+1)]^{1/2} \delta_{m0}$$

where in the last step the orthogonality property of the 3-j symbols is used [34]:

$$\sum_{\lambda\mu} (2\lambda+1) \begin{pmatrix} l & l' & \lambda \\ m_1 & m_2 & \mu \end{pmatrix} \begin{pmatrix} l & l' & \lambda \\ p_1 & p_2 & \mu \end{pmatrix} = \delta_{m_1 p_1} \delta_{m_2 p_2}.$$

Thus,

$$\bar{B}_{lm} \approx -\frac{e^{i\omega d}}{\omega d} \sqrt{(2l+1)} \sum_{l'} B_{l'0} i^{l'} \sqrt{(2l'+1)} \delta_{m0} = -\frac{e^{i\omega d}}{\omega d} \sqrt{(2l+1)} T(B_{l0}) \delta_{m0},$$

where, for X_l being any function of l , the functional $T(X_l)$ is defined as:

$$T(X_l) \triangleq \sum_{l'} X_{l'} i^{l'} \sqrt{(2l'+1)}$$

If $m \neq 0$; $B_{lm} = E_{lm}$, $C_{lm} = F_{lm}$ and if $m = 0$:

$$\begin{aligned} B_{l0} &= -e^{i\omega\tau} \frac{e^{i\omega d}}{\omega d} (-1)^l \sqrt{(2l+1)} \gamma_l^-(\omega a) T(B_{l0}) + \frac{e^{i\omega d}}{\omega d} (-1)^l \sqrt{(2l+1)} \gamma_l^+(\omega a) T(C_{l0}) + E_{l0}, \\ C_{l0} &= -e^{-i\omega\tau} \frac{e^{i\omega d}}{\omega d} (-1)^l \sqrt{(2l+1)} \gamma_l^-(\omega a) T(C_{l0}) + \frac{e^{i\omega d}}{\omega d} (-1)^l \sqrt{(2l+1)} \gamma_l^+(\omega a) T(B_{l0}) + F_{l0}. \end{aligned}$$

Multiplying each side of these equations by $i^l \sqrt{(2l+1)}$ and summing over l gives $T(B_{l0})$ and $T(C_{l0})$:

$$\begin{bmatrix} T(B_{l0}) \\ T(C_{l0}) \end{bmatrix} = \begin{bmatrix} 1 - e^{i\omega\tau} \frac{e^{i\omega d}}{\omega d} T((-i)^l (2l+1) \gamma_l^-(\omega a)) & \frac{e^{i\omega d}}{\omega d} T((-i)^l (2l+1) \gamma_l^+(\omega a)) \\ \frac{e^{i\omega d}}{\omega d} T((-i)^l (2l+1) \gamma_l^+(\omega a)) & 1 - e^{-i\omega\tau} \frac{e^{i\omega d}}{\omega d} T((-i)^l (2l+1) \gamma_l^-(\omega a)) \end{bmatrix}^{-1} \begin{bmatrix} T(E_{l0}) \\ T(F_{l0}) \end{bmatrix}$$

$a \ll 1$:

Similar to the 2+1 dimensional case, for $a \ll 1$, $\gamma_l^\pm(\omega a)$ becomes a discrete delta function, δ_l . Due to the factors of $\gamma_l^\pm(\omega a)$ in each term, B_{lm} and C_{lm} are nonzero for only $l = m = 0$. The problem reduces to finding the constants B_{00} and C_{00} .

$$\gamma_l^+(\omega a) \approx \gamma_l^-(\omega a) \approx \frac{\omega a}{i + \omega a} \delta_l,$$

$$\begin{aligned} B_{lm} &= B_{00} \delta_l \delta_m, \\ C_{lm} &= C_{00} \delta_l \delta_m. \end{aligned}$$

$l = 0$ implies $m = 0$ and $l' = \lambda$, so that

$$\begin{aligned} \bar{B}_{00} &= \sum_{\lambda} B_{00} \delta_{\lambda} c(\lambda 0 | 00 | \lambda 0) h_{\lambda}^{(1)}(\omega d) \sqrt{\frac{2\lambda + 1}{4\pi}} = B_{00} h_0^{(1)}(\omega d), \\ \bar{C}_{00} &= \sum_{\lambda} C_{00} \delta_{\lambda} c(\lambda 0 | 00 | \lambda 0) h_{\lambda}^{(1)}(\omega d) (-1)^{\lambda} \sqrt{\frac{2\lambda + 1}{4\pi}} = C_{00} h_0^{(1)}(\omega d). \end{aligned}$$

B_{00} and C_{00} are found as:

$$\begin{bmatrix} B_{00} \\ C_{00} \end{bmatrix} = \begin{bmatrix} 1 - e^{i\omega\tau} h_0^{(1)}(\omega d) & h_0^{(1)}(\omega d) \\ h_0^{(1)}(\omega d) & 1 - e^{-i\omega\tau} h_0^{(1)}(\omega d) \end{bmatrix}^{-1} \begin{bmatrix} E_{00} \\ F_{00} \end{bmatrix}.$$

Multiple scattering

Multiple scattering formulae for the 3+1 dimensions can be found by the same steps followed as the 2+1 dimensional case. The multiple scattering expansion of 3+1 dimensional wave functions are:

$$\begin{aligned}\Psi_1^k &= \sum_{lm} B_{lm}^k \cdot h_l^{(1)}(\omega r) Y_{lm}(\theta, \varphi), \\ \Psi_2^k &= \sum_{lm} C_{lm}^k \cdot h_l^{(1)}(\omega R) Y_{lm}(\Theta, \varphi),\end{aligned}$$

The wormhole conditions for the 1^{st} and the k^{th} order scattering coefficients for 3 dimensional case are:

$$\begin{aligned}(\Psi_0 + \Psi_1^1)_{r=a} &= e^{i\omega\tau} (\Psi_0 + \Psi_2^1)_{R=a, \Theta=\theta}, \\ \frac{\partial}{\partial r} (\Psi_0 + \Psi_1^1)|_{r=a} &= -e^{i\omega\tau} \frac{\partial}{\partial R} (\Psi_0 + \Psi_2^1)|_{R=a, \Theta=\theta}, \\ (\Psi_1^{k+1} + \Psi_2^k)|_{r=a} &= e^{i\omega\tau} (\Psi_1^k + \Psi_2^{k+1})|_{R=a, \Theta=\theta}, \\ \frac{\partial}{\partial r} (\Psi_1^{k+1} + \Psi_2^k)|_{r=a} &= -e^{i\omega\tau} \frac{\partial}{\partial R} (\Psi_1^k + \Psi_2^{k+1})|_{R=a, \Theta=\theta},\end{aligned}$$

When the 1^{st} and the k^{th} order scattering coefficients satisfies the wormhole conditions, total wave satisfies wormhole conditions as well:

$$\begin{aligned}\Psi|_{r=a} &= (\Psi_0 + \Psi_1 + \Psi_2)|_{r=a} = (\Psi_0 + \Psi_1^1 + \sum_{k=1}^{\infty} (\Psi_1^{k+1} + \Psi_2^k))|_{r=a} \\ &= e^{i\omega\tau} (\Psi_0 + \Psi_2^1)|_{R=a, \Theta=\theta} + e^{i\omega\tau} \sum_{k=1}^{\infty} (\Psi_1^k + \Psi_2^{k+1})|_{R=a, \Theta=\theta} = e^{i\omega\tau} (\Psi_0 + \Psi_1 + \Psi_2)|_{R=a, \Theta=\theta}.\end{aligned}$$

Wormhole conditions for the 1^{st} order coefficients gives:

$$\begin{aligned}
& \sum_{lm} A_{lm} j_l(\omega a) Y_{lm}(\theta, \varphi) + B_{lm}^1 \cdot h_l^{(1)}(\omega a) Y_{lm}(\theta, \varphi) \\
& = e^{i\omega\tau} \left(\sum_{lm} \bar{A}_{lm} j_l(\omega a) Y_{lm}(\theta, \varphi) + \sum_{lm} C_{lm}^1 h_l^{(1)}(\omega a) Y_{lm}(\theta, \varphi) \right),
\end{aligned}$$

Equating the coefficients of $Y_{lm}(\theta, \varphi)$ for each l, m :

$$B_{lm}^1 - e^{i\omega\tau} C_{lm}^1 = -\frac{j_l(\omega a)}{h_l^{(1)}(\omega a)} (A_{lm} - e^{i\omega\tau} \bar{A}_{lm}). \quad (3.3.46)$$

$$\begin{aligned}
& \sum_{lm} A_{lm} j_l(\omega a) Y_{lm}(\theta, \varphi) + B_{lm}^1 \cdot h_l^{(1)}(\omega a) Y_{lm}(\theta, \varphi) \\
& = e^{i\omega\tau} \left(\sum_{lm} \bar{A}_{lm} j_l(\omega a) Y_{lm}(\theta, \varphi) + \sum_{lm} C_{lm}^1 h_l^{(1)}(\omega a) Y_{lm}(\theta, \varphi) \right),
\end{aligned}$$

gives a second equation similar to (3.3.46)

$$B_{lm}^1 + e^{i\omega\tau} C_{lm}^1 = -\frac{\frac{\partial}{\partial r} j_l(\omega a)}{\frac{\partial}{\partial r} h_l^{(1)}(\omega a)} (A_{lm} + e^{i\omega\tau} \bar{A}_{lm}). \quad (3.3.47)$$

Solving B_{lm}^1 and C_{lm}^1 gives:

$$B_{lm}^1 = -\gamma_l^+(\omega a) A_{lm} + e^{i\omega\tau} \gamma_l^-(\omega a) \bar{A}_{lm}, \quad (3.3.48)$$

$$C_{lm}^1 = -\gamma_l^+(\omega a) \bar{A}_{lm} + e^{-i\omega\tau} \gamma_n^-(\omega a) A_{lm}. \quad (3.3.49)$$

and k^{th} order scattering coefficients are found similarly as:

$$\begin{aligned}
B_{lm}^{k+1} &= -\gamma_l^+(\omega a)\bar{C}_{lm}^k + e^{i\omega\tau}\gamma_n^-(\omega a)\bar{B}_{lm}^k, \\
C_{lm}^{k+1} &= -\gamma_l^+(\omega a)\bar{B}_{lm}^k + e^{-i\omega\tau}\gamma_n^-(\omega a)\bar{C}_{lm}^k.
\end{aligned}$$

3.4 Numerical verification of the solution:

In this section, the solutions for certain values of a , d , ω and τ are evaluated numerically for 2+1 dimensions and it is verified that they satisfy wormhole conditions. Numerical evaluation of solutions are done by using the multiple scattering results (3.2.29), (3.2.30), (3.2.31) and (3.2.32). Alternatively (3.2.17) and (3.2.18) are tested by an iteration method. For iteration, two initial test functions B_n^0 and C_n^0 are picked and substituted to right hand sides of (3.2.17) and (3.2.18) to obtain B_n^1 and C_n^1 . Similarly B_n^1 and C_n^1 are substituted to (3.2.17) and (3.2.18) to obtain B_n^2 and C_n^2 . Continuing this iteration, B_n^m and C_n^m are assumed to converge to the solution. No proof for the conditions of convergence is given, it is verified numerically that the solution found by iteration method converges to the multiple scattering solution for the parameter sets that are considered.

Moreover, to check the formulas found for $a \ll d$ the solutions found by this method is compared with the multiple scattering solution.

As the velocity of wave is taken as 1 in equation (3.1.1), $\omega d = 2\pi d/\lambda$ and $\omega a = 2\pi a/\lambda$ where λ is the wavelength of the wave. Practically if when a light wave in a wormhole universe is considered, these values supposed to be much larger (at least order of $\sim 10^{10}$) compared to what chosen in the below examples. However, numerical calculations with such large values were beyond the capacity of the PC used and there is no reason to think that the formulas will fail for large values.

The incident wave Ψ_0 is chosen as a plane wave and $A_n = e^{in\alpha}$, where α is the angle between direction of the incident wave and the y axis.

Referring to figure 3.2, the wormhole is located symmetrically with respect to the y axis. Consider the reflection operator R with respect to the y axis, i.e. $R\Psi(x, y) =$

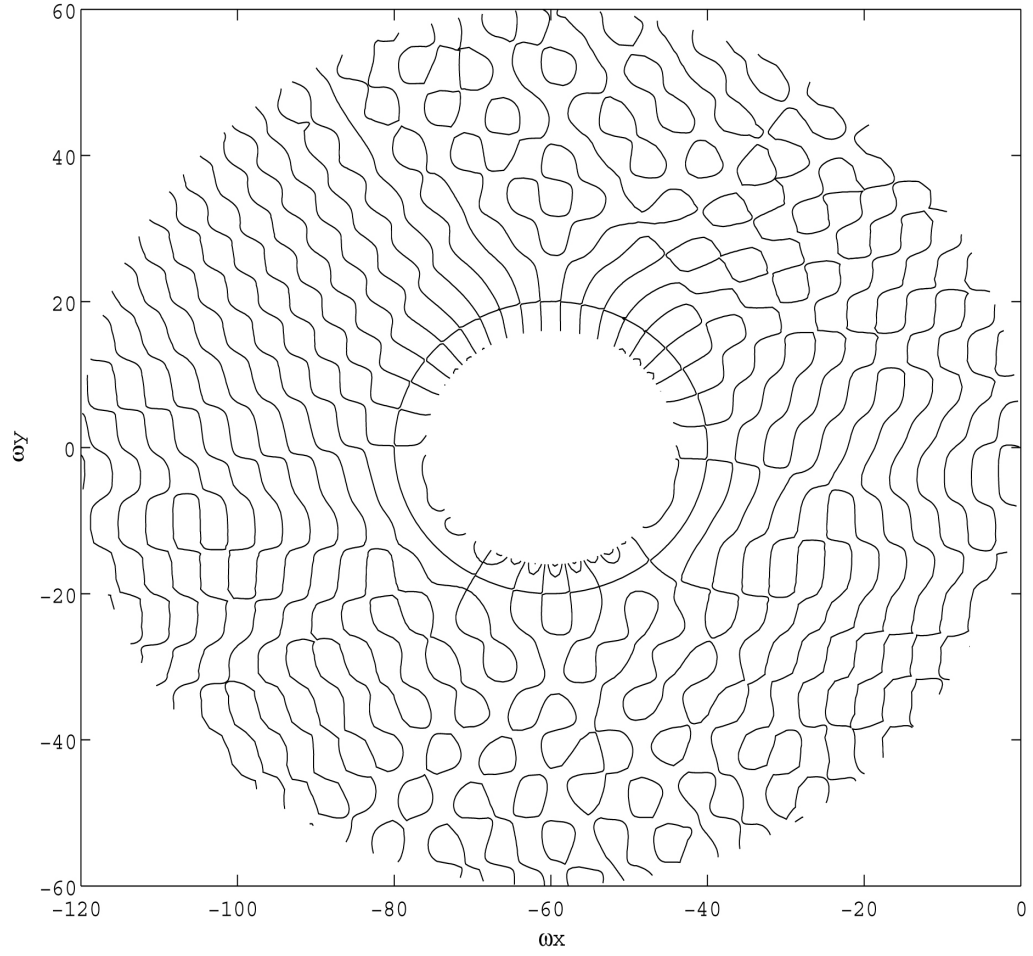


Figure 3.4: The contour plot of $\text{Re}(\Psi - e^{i\omega\tau}R\Psi)$ in the vicinity of left wormhole mouth Δ_- . The contour circle at $r = a$ shows that $(\Psi - e^{i\omega\tau}R\Psi)|_{r=a}$ is constant. ($\omega a = 20$; $\omega d = 120$; $\tau = 1$; $\alpha = \pi/3$)

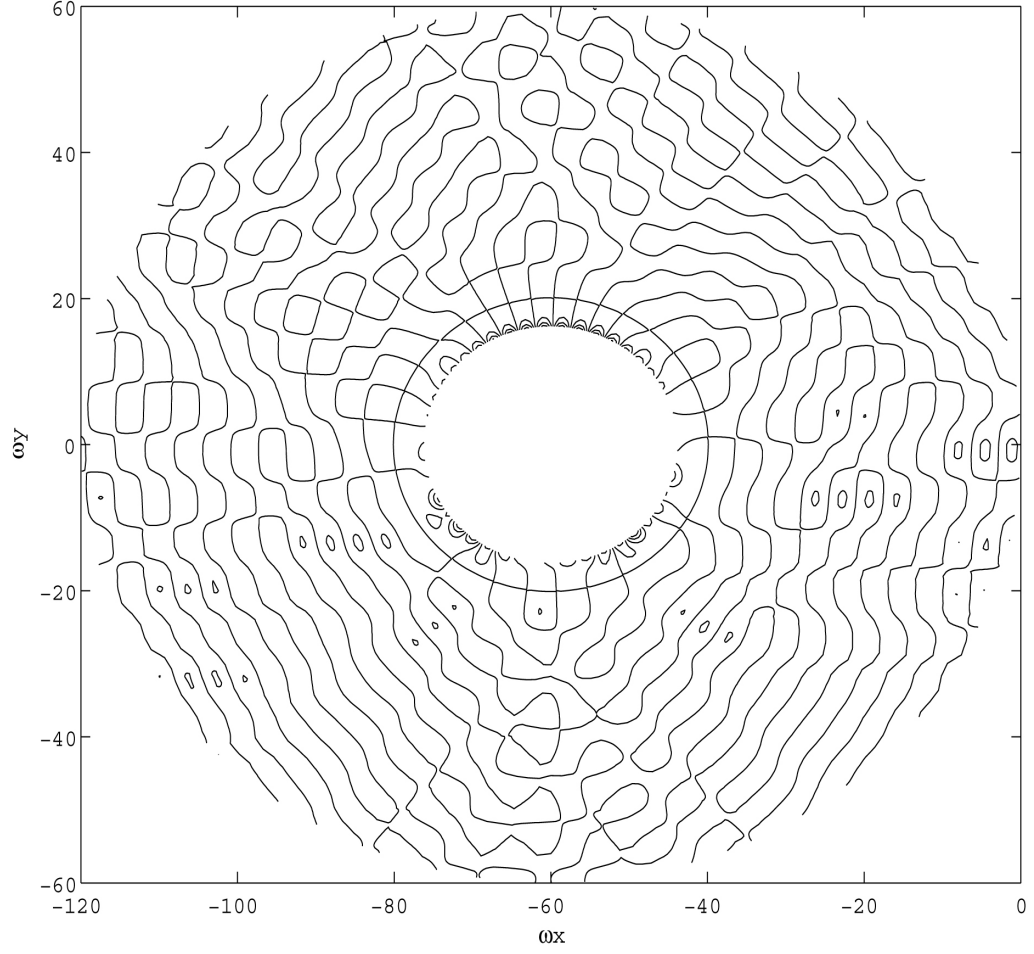


Figure 3.5: The contour plot of $\text{Re}(\frac{\partial}{\partial r}(\Psi + e^{i\omega\tau}R\Psi))$ in the vicinity of left wormhole mouth Δ_- . The same contour circle at $r = a$ is evident. ($\omega a = 20$; $\omega d = 120$; $\tau = 1$; $\alpha = \pi/3$)

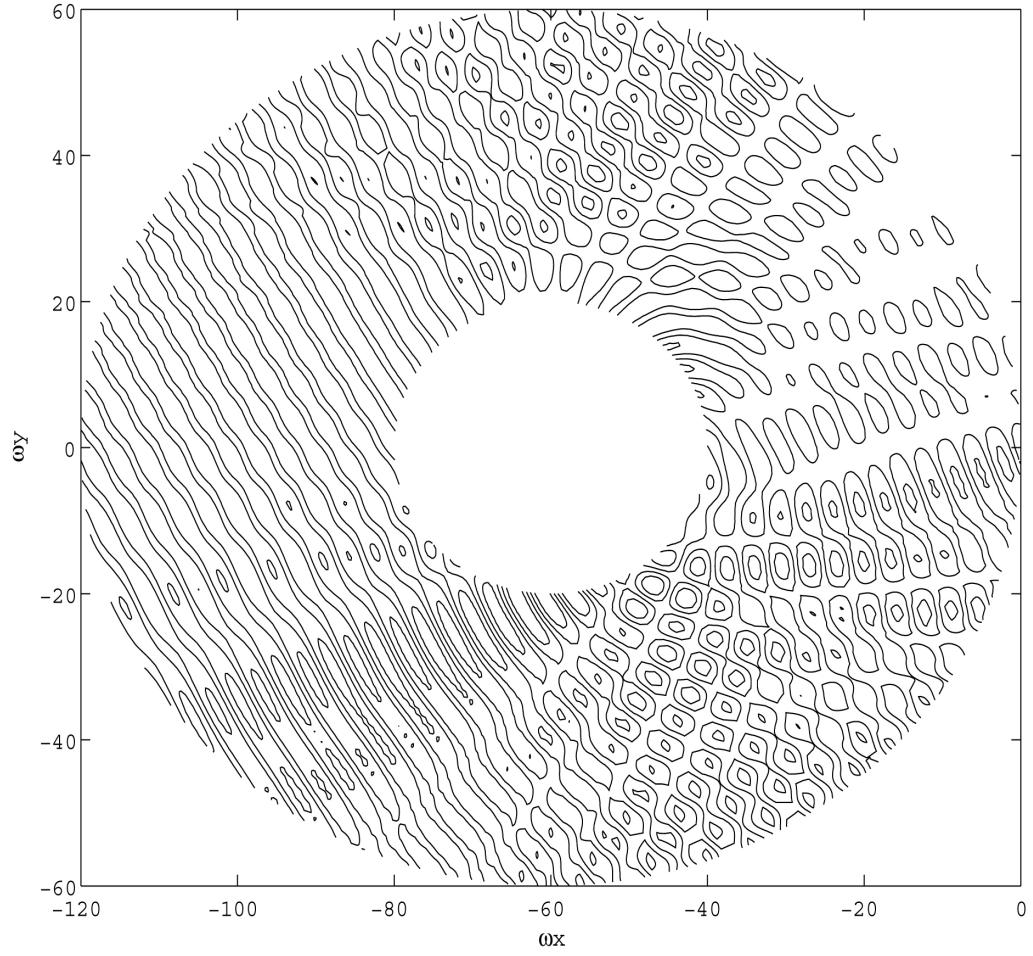


Figure 3.6: The contour plot of $\text{Re}(\Psi)$ in the vicinity of Δ_- . The incident wave is coming from the left with an angle $\pi/3$ and the shadow is on the opposite side. ($\omega a = 20$; $\omega d = 120$; $\tau = 1$; $\alpha = \pi/3$).

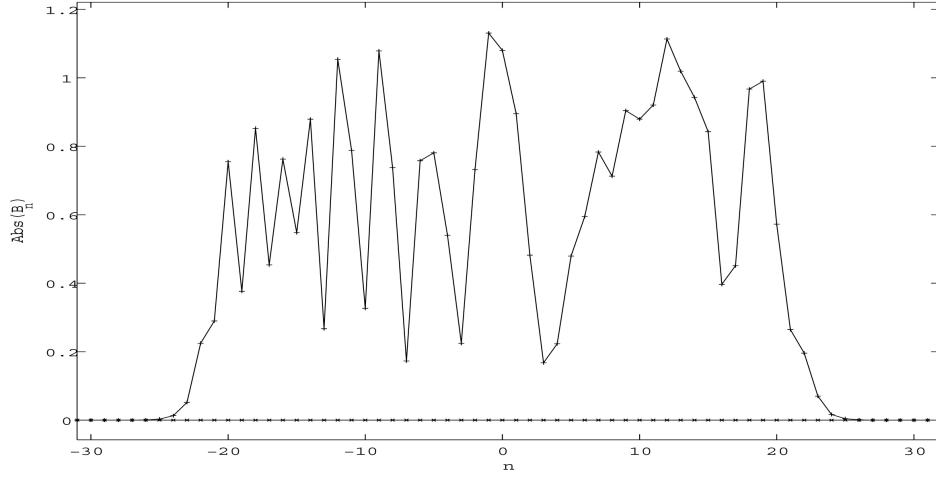


Figure 3.7: Comparison of the multiple scattering and the iteration results. The difference of $|B_n|$ found by these two methods are points with marker 'x' which are zero for all n . ($\omega a = 20$; $\omega d = 120$; $\tau = 1$; $\alpha = \pi/3$)

$\Psi(-x, y)$. According to the wormhole conditions C-1 and C-2

$$(\Psi - e^{i\omega\tau} R\Psi)|_{r=a} = 0 \quad (3.4.50)$$

$$\frac{\partial}{\partial r}(\Psi + e^{i\omega\tau} R\Psi)|_{r=a} = 0 \quad (3.4.51)$$

It is verified that the solution found satisfies (3.4.50) and (3.4.51) by plotting the contours at the vicinity of one of the wormhole mouths.

In Figure 3.4, figure 3.5, figure 3.6 and figure 3.7 the parameters are: $\omega a = 20$, $\omega d = 120$, $\alpha = \pi/3$, $\omega\tau = 1$. Figure 3.4 and figure 3.5 show contour plots of the multiple scattering solution for real part of $\Psi(x, y) + e^{i\omega\tau} R(\Psi(x, y))$ and $\frac{\partial}{\partial r}(\Psi(x, y) - e^{i\omega\tau} R(\Psi(x, y)))$, respectively. In both figures, the contour circles at $\omega r = \omega a = 20$ are clearly visible indicating that the values of each function are zero along $r = a$ circle. This shows that the wormhole conditions are satisfied. The contour plots of imaginary parts -which are not presented here- give the same contour circles at $r = a$. Although the contour is plotted for $0.8a < r < d$ to make the zero contour

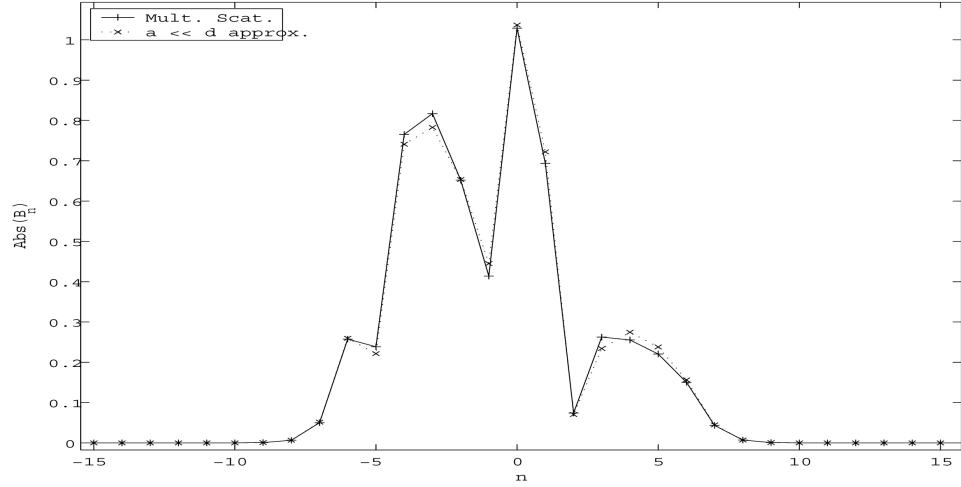


Figure 3.8: Comparison of the multiple scattering and the $a \ll d$ approximation. ($\omega a = 5$; $\omega d = 1600$; $\omega \tau = 1$; $\alpha = \pi/5$)

circle more visible, it should be remembered that the region $r < a$ is not a part of the spacetime. Figure 3.6 is a contour plot of the real part of the solution $\Psi(r, \theta)$ to give an example of a visual image of the solution. Figure 3.7 is a comparison of the multiple scattering solution and the iteration solution. The solid line with ‘+’ markers show the $|B_n|$ that are found by multiple scattering and dashed line with ‘x’ markers are the difference of the absolute values of B_n found by the iteration method and the multiple scattering method. The difference is zero for all n ; i.e. these two solutions are exactly the same. The results are obtained after 20 iterations. The test functions are chosen as constant, $B_n^0 = C_n^0 = 1$.

In figure 3.8, the parameters are: $\omega a = 5$, $\omega d = 1600$, $\alpha = \pi/5$, $\omega \tau = 1$. This is an example for $a \ll d$ case. In the figure $|B_n|$ versus n is plotted. The solid line with ‘+’ markers is the multiple scattering solution and the dashed line with ‘x’ markers is the $a \ll d$ approximation solutions given by (3.2.22) and (3.2.23).

3.5 Dependence of the scattered waves to wormhole parameters

In this section, the results found for scattered wave solutions from a 2+1 dimensional wormhole will be explored for different time lag τ , incidence angle α , and wormhole parameters a , d . The results will be compared with that of a conducting sphere of radius equal to radius of wormhole throat. The parameter that distinguishes the wormhole from an ordinary globally hyperbolic manifold with an handle is the time lag τ . First the solutions with different τ are compared.

Effect of τ :

Since τ enters to the equations as $\exp(i\omega\tau)$, the important quantity is $\omega\tau$ instead of τ . $\exp(i\omega\tau)$ being periodic with 2π , it is sufficient to consider the effect of $\omega\tau$ in the range $0 \leq \omega\tau \leq 2\pi$. The coefficients B_n and C_n are obtained for $\omega\tau = 0$, $\omega\tau = \pi/2$ and $\omega\tau = \pi$. The other parameters are kept constant: ($\omega a = 15$, $\omega d = 200$, $\alpha = 0$).

The geometry of the 2+1 dimensional wormhole has mirror symmetry along y axis. When the incidence angle α is zero, the incident wave is symmetrical along y axis also, and the solution will be symmetrical as well. On the contrary when the incidence angle is $\pi/2$, the left wormhole mouth will shadow the right mouth and symmetry will be lost like any other nonzero incidence angle. Therefore for $\alpha = 0$, due to symmetry B_n is equal to C_n . When $\alpha \neq 0$, changing α to $-\alpha$ interchanges the role of B_n and C_n . Therefore only B_n is plotted.

The magnitude of B_n for three different values of $\omega\tau$ is shown in figure 3.8. It is seen that the coefficients for $n > \omega a$ vanishes rapidly as usual, and for the lower values of n , the envelope of the magnitudes are almost uniform. But at the sides of the spectrum, there exist one last smaller peak for $\omega\tau = 0$, and this peak fades away as $\omega\tau$ deflects from zero. The same pattern is observed for another set of parameters: $\omega a = 60$, $\omega d = 180$, $\alpha = 0$ with α unchanged (Figure 3.9).

The phase of B_n does not seem to give any significant information and not plotted. In Figure 3.10 is an example for $\alpha \neq 0$ case. $\alpha = \pi/3$; $\omega a = 30$, $\omega d = 300$.

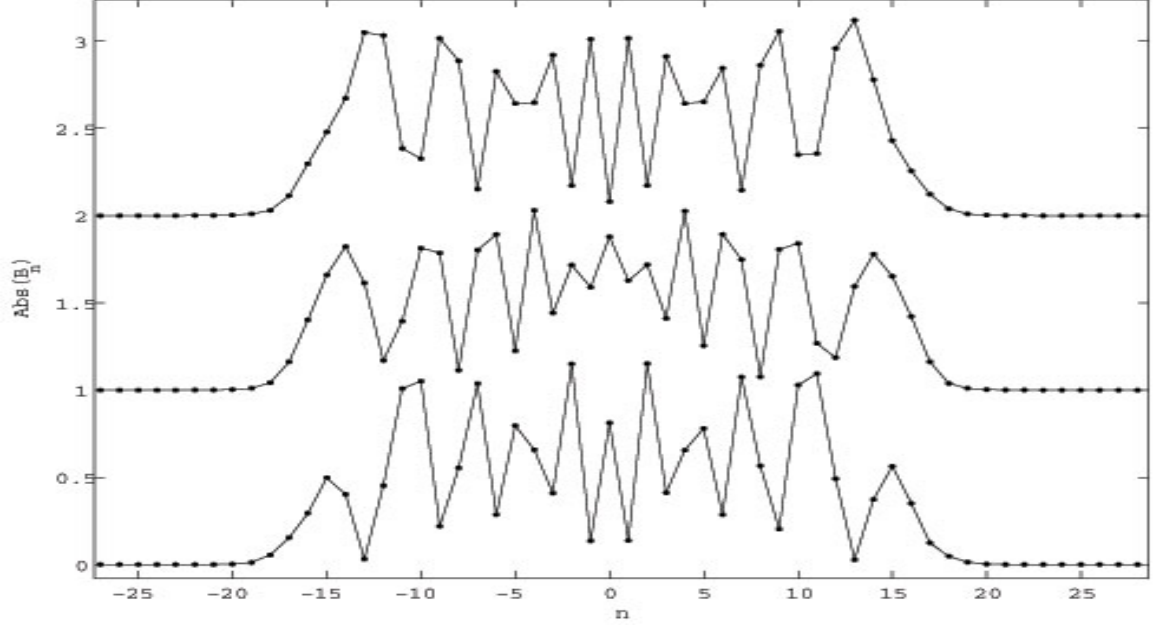


Figure 3.9: Scattering coefficients for different $\omega\tau$ values: From above to below $\omega\tau$ values are π , $\pi/2$ and 0, respectively. ($\omega a = 15$, $\omega d = 200$, $\alpha = 0$).

The contour plot of the real part of the total wave for $\tau = 0$, $\tau = \pi/2$ and $\tau = \pi$ are shown in Figure 3.11, Figure 3.12 and Figure 3.13. It is interesting that the wormhole mouth completely shadows the incident wave and the total wave is almost zero in the shadowed region. Different set of a and d confirms this observation. The shadow effect is most strong for $\tau = \pi$. We have no theoretical explanation so far for this observation. Not only the real part, imaginary part of the total wave is also zero in the shadow region. This situation is not specific to $\alpha = 0$; the same phenomena is observed in different incident wave directions.

Comparison of the small d/a and large d/a cases.

To observe the effect of moving apart the wormholes mouths, the scattered wave coefficients are calculated for two different parameter set. The radius of the throat a is kept constant and d is increased. Figure 3.14 shows the $\alpha = 0$ case and Figure 3.15 shows $\alpha = \pi/3$ case.

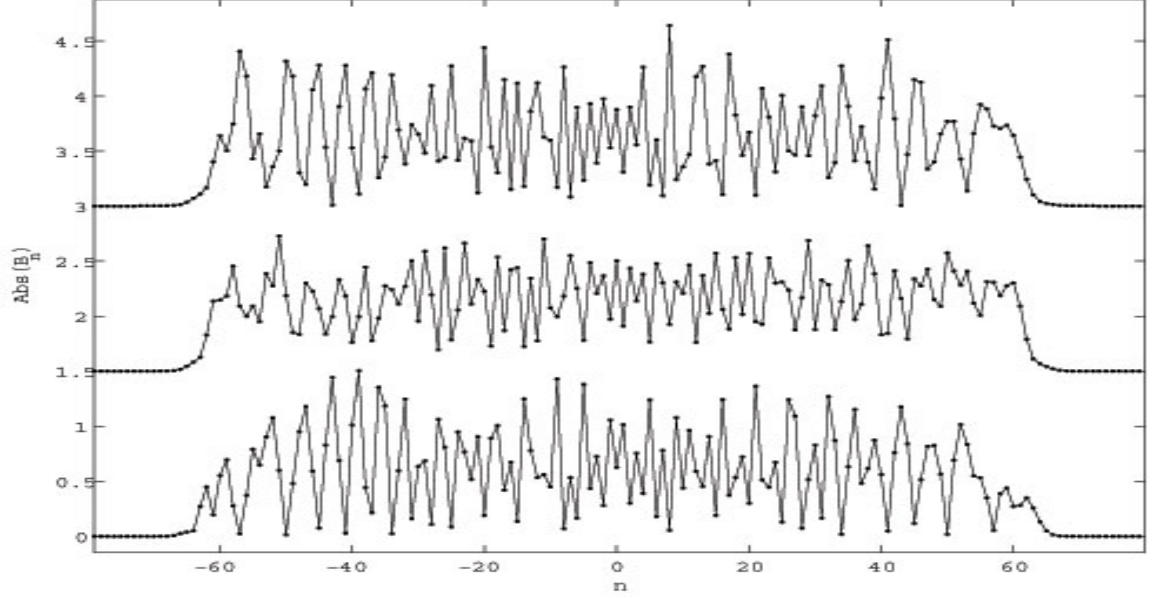


Figure 3.10: From above to below, $\omega\tau$ values are again π , $\pi/2$ and 0, respectively. ($\omega a = 60$, $\omega d = 180$, $\alpha = 0$).

3.6 Comparison with the scattering from a conducting cylinder:

The problem of scattering from a wormhole that admit closed timelike curves is handled identical to scattering from an arbitrary object. The topology of the space-time itself can be viewed as an scatterer object. If there were a real wormhole in the universe it would be possible to obtain the radar image of the wormhole by sending waves and measuring the reflected wave. Considering that the wormhole studied in this thesis is cylindrical (or spherical for 3+1 dimensional case), the coefficients of scattering from a cylindrical object satisfying Dirichlet boundary conditions on its surface can be compared with that of wormhole.

The expression for an incident plane wave making an angle α with y axis is:

$$e^{i\omega r \sin(\alpha-\theta)} = \sum_{n=-\infty}^{n=\infty} e^{-in\alpha} J_n(\omega r) e^{in\theta} \quad (3.6.52)$$

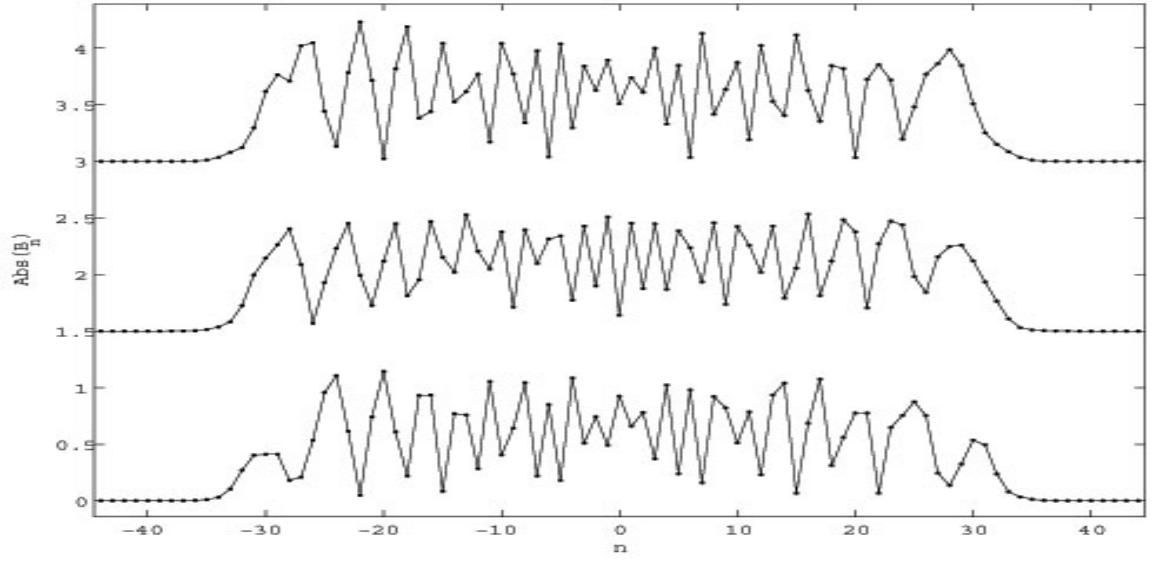


Figure 3.11: $\alpha = \pi/3$. $\omega\tau$ values are again π , $\pi/2$ and 0, respectively from above to below. ($\omega a = 30$, $\omega d = 300$).

The scattered wave can be expressed as:

$$\Psi_s(r, \theta) = \sum_{n=-\infty}^{n=\infty} D_n H_n^{(1)}(\omega r) e^{in\theta} \quad (3.6.53)$$

Applying the Dirichlet boundary condition at $r = a$ gives:

$$D_n = -\frac{e^{-in\alpha} J_n(\omega a)}{H_n^{(1)}(\omega a)} \quad (3.6.54)$$

The magnitudes of B_n and D_n are shown in figure 3.16 where $\omega a = 20$, $\omega d = 80$, $\tau = 0$, $\alpha = \pi/3$. Figure also shows $\omega\tau = \pi$ case. The coefficients B_n and D_n , both vanishes rapidly for $n > \omega a$ and their pattern are similar in this sense.

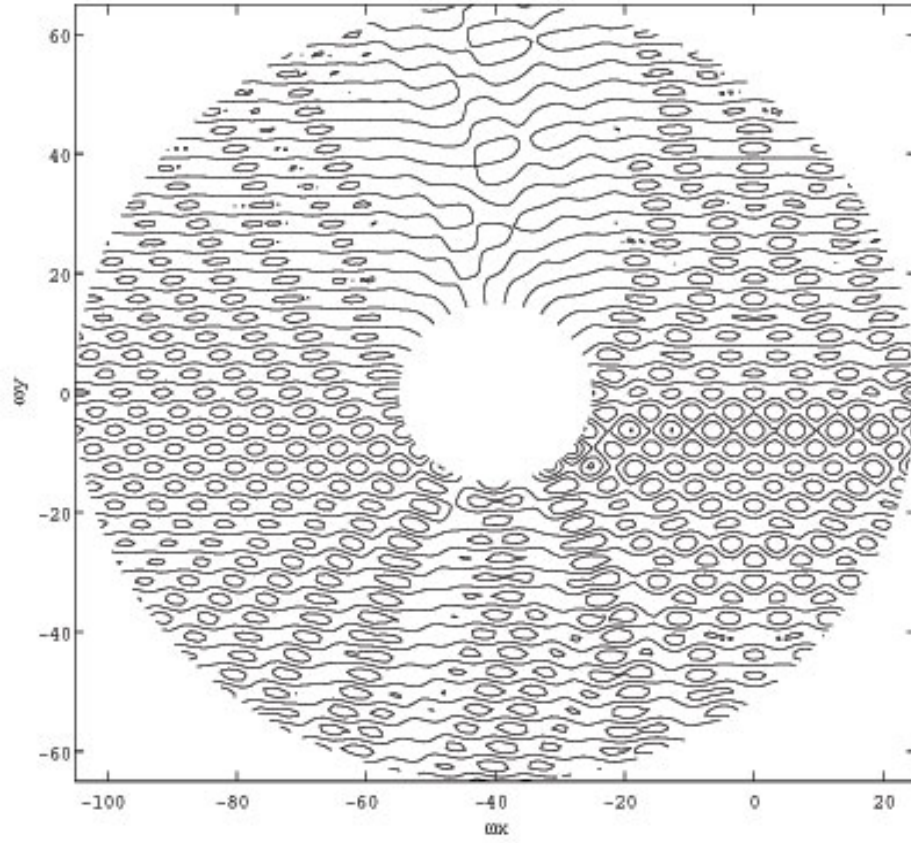


Figure 3.12: The Contour plot of the total wave around left wormhole mouth for $\omega\tau = 0$. ($\omega a = 15$, $\omega d = 40$, $\alpha = 0$)

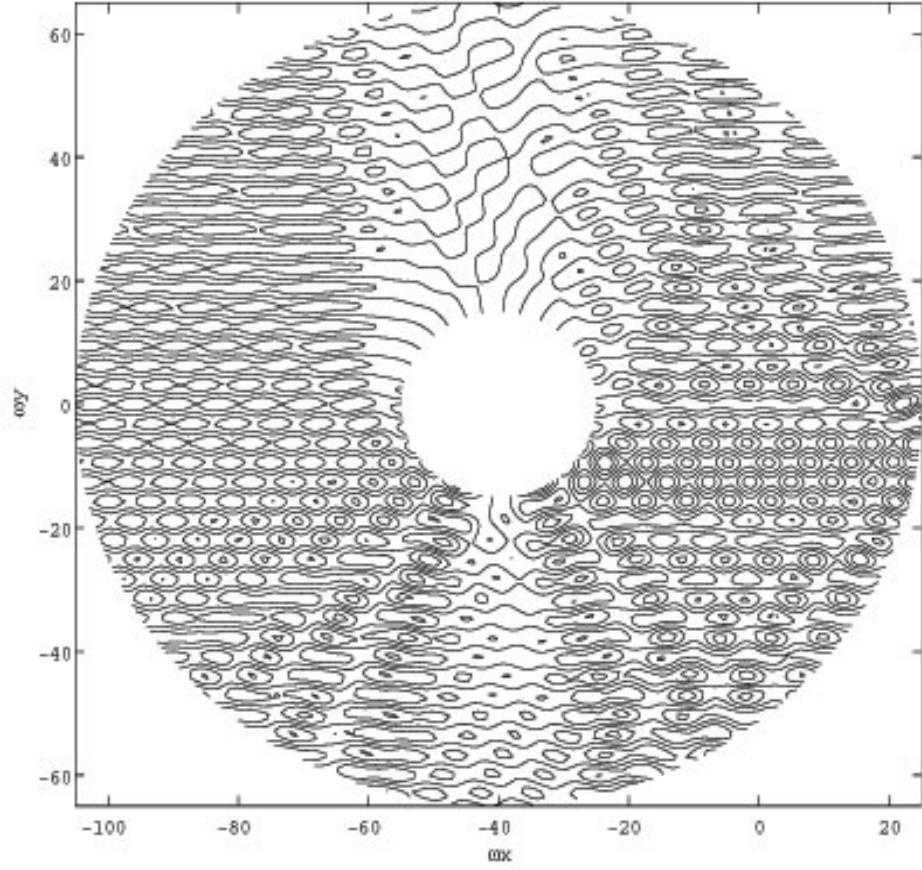


Figure 3.13: The Contour plot of the total wave around left wormhole mouth for $\omega\tau = \pi/2$. ($\omega a = 15$, $\omega d = 40$, $\alpha = 0$)

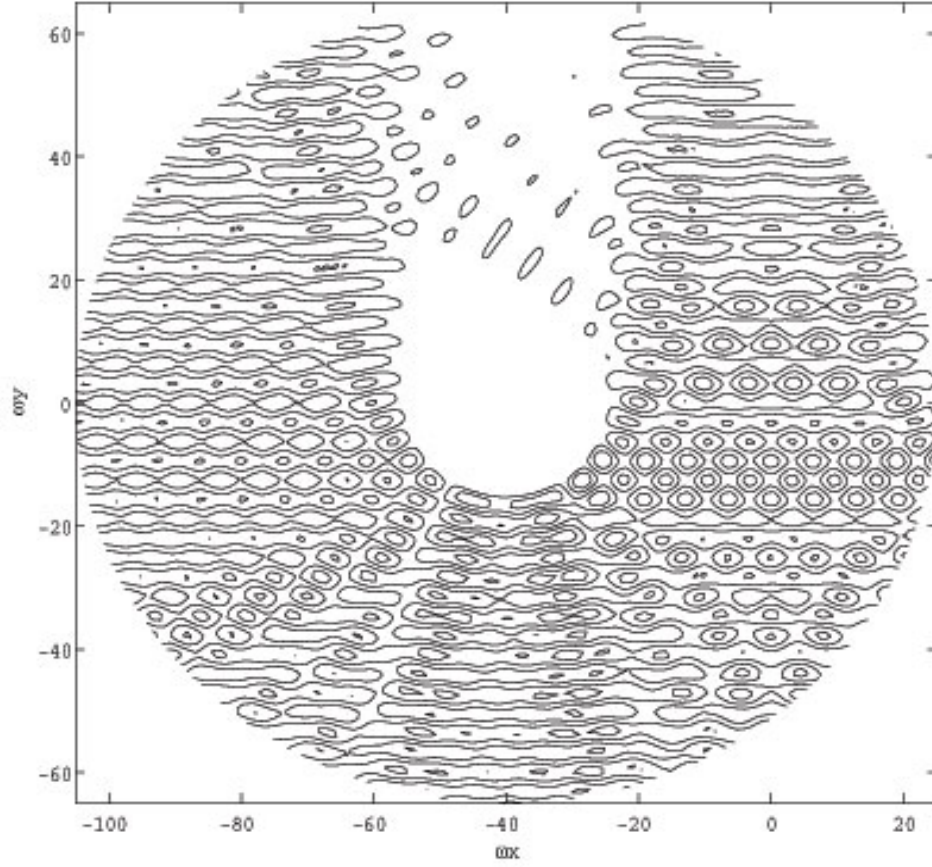


Figure 3.14: The Contour plot of the total wave around left wormhole mouth for $\omega\tau = \pi$. The effect of the shadow at upper part of the wormhole mouth shows itself stronger than othe $\omega\tau$ values. ($\omega a = 15$, $\omega d = 40$, $\alpha = 0$)

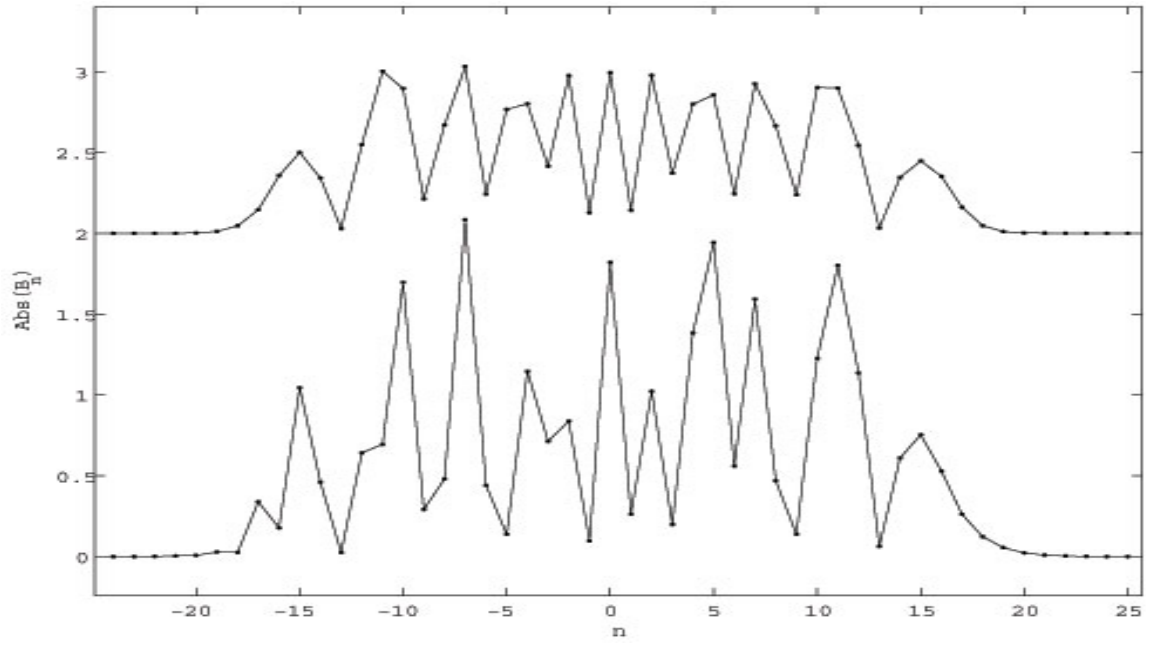


Figure 3.15: Below: $\omega a = 15, \omega d = 1600$; above: $\omega a = 15, \omega d = 30.02$. ($\alpha = 0$)

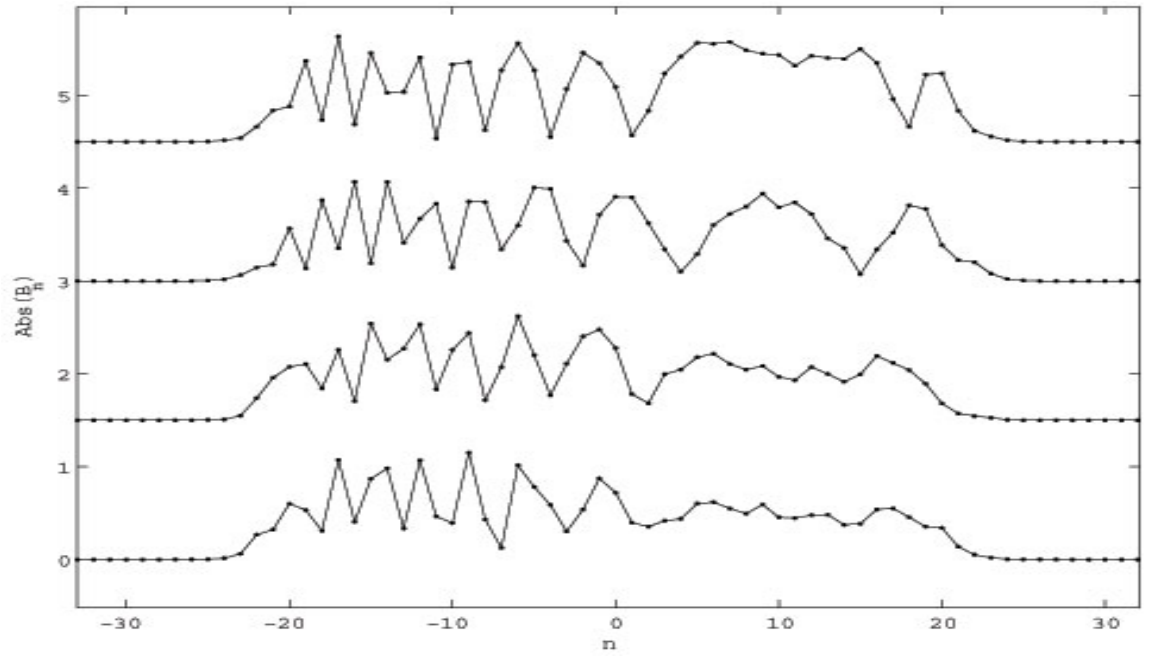


Figure 3.16: From above to below, $\omega d = 500$, $\omega d = 200$, $\omega d = 50$ and $\omega d = 42$ respectively. ($\omega a = 15$, $\alpha = \pi/3$).

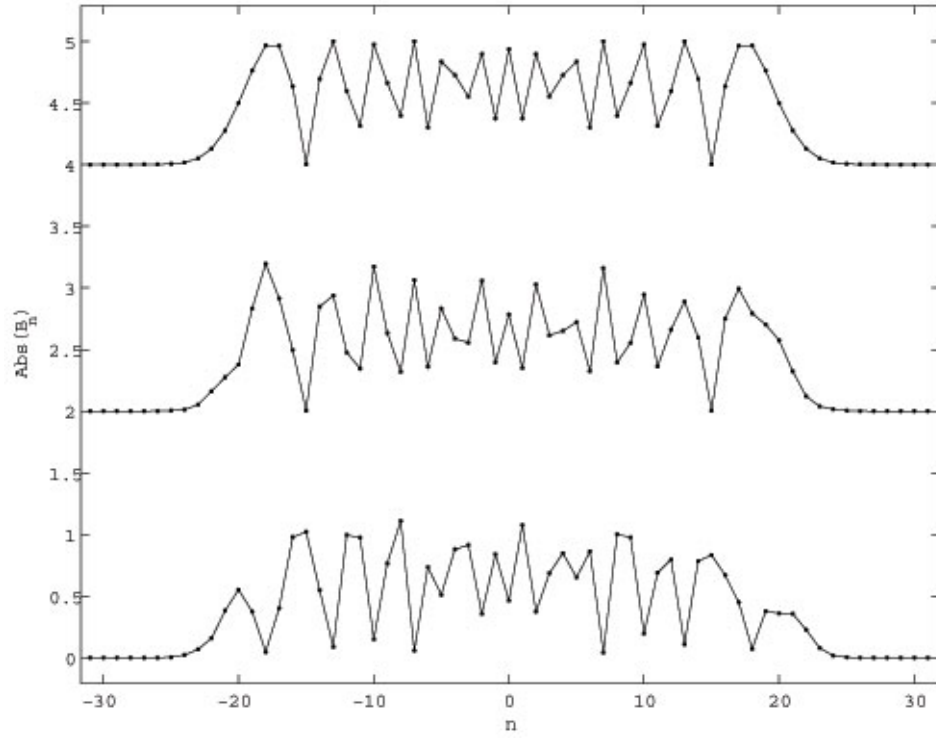


Figure 3.17: From above to below: (1) conducting sphere. (2) wormhole: $\omega\tau = \pi$; (3) wormhole: $\omega\tau = 0$; ($\omega a = 20, \omega d = 80, \alpha = 0$)

CHAPTER 4

CONCLUSIONS

The principal purpose of the present work was to investigate the properties of scalar waves in chronology violating spacetimes and specifically in a wormhole topology.

The principal results can be summarized as follows: Existence of closed timelike curves may force the solution of the wave equation to be composed of frequencies from a discrete set: Not all the frequencies which form a continuum can exist as the solution, instead only certain frequencies that constitute a discrete set are allowed.

However, this is not true for all spacetimes that admit closed timelike curves. In the wormhole spacetime analysed in section III, there is no restriction on the frequency of the waves. The main difference between the spacetimes studied in section II (which has the frequency selection property) and wormhole spacetime is that in wormhole spacetime, the region of the spacetime that closed null curves are confined to a set of measure zero in the spacetime. It can be conjectured that if a spacetime admits closed null curves and if these curves are not confined to a set of measure zero within the spacetime the solution of the wave equation has frequency selection property.

On the other hand frequency selection is not specific to spacetimes admitting closed timelike curves; the results of Chapter II.A shows that product manifolds whose space component is compact may also have the same property. Thus it seems that there is no anomaly specific to existence of closed timelike curves.

Although the wormhole spacetime considered in this work admits CTCs for sufficiently large values of time lag τ , their existence has no influence on monochromatic waves. The closed timelike curves emerge when time lag τ is greater than $d - 2a$. However, τ appears in the equations only as $\exp(i\omega\tau)$. Thus the solution remains

the same for all integer k 's where $\omega\tau = 2k\pi + \alpha$ and increasing τ does not change the nature of the solutions. This suggests that the presence of closed timelike curves does not have a dramatic effect on the scalar wave solutions.

This should not be surprising considering that, in a wave equation, what really matters is presence of closed null curves, rather than closed timelike curves. It is reasonable to think that the existence of closed timelike curves will not effect the nature of the solutions as long as closed null curves are not present. CTC's are present in the flat wormhole spacetime studied here, but still they don't have a significant effect on the solution. The reason is explained in [17]: In this kind of spacetimes, the closed null curves are a set of measure zero and due to the diverging lens property of the wormhole, the strength of the field is weakened by a factor $a/2d$ at each loop in the infinitely looping closed null geodesics [35],[36].

The complications related to closed timelike curves are due to difficulty in specifying a Cauchy hypersurface when solving the Cauchy problem. Null geodesics are bicharacteristics of the wave equation and arbitrary initial data cannot be properly posed in a null direction [1]. A spacelike hypersurface never contains vectors in a null direction, thus are good candidates for specifying initial data. However there always exist a null direction on a timelike point of a hypersurface. In the light of these discussions it can be conjectured that no complications arise on the solution of wave equation due to CTC's. The complications are mainly due to the nature of Cauchy problem approach.

If we consider the question in a purely mathematical point of view, the form of the wave equation considered is almost symmetric with respect to time and space variables. For the 1+1 dimensions there is complete symmetry (remembering that the minus sign on the time derivative does not effect the symmetry since it is always possible to reverse the signs) and for higher dimensions the only difference is having more space variables. This suggest that there is no strong mathematical background for expecting disparate consequences of existence of CTC's compared to existence of closed curves along any space direction. On the other hand more space coordinates give rise to asymmetry between the spacelike hypersurfaces and the timelike hypersurfaces in Cauchy problem due to the shape of the null cone: Any timelike hypersurface passing through a spacetime point intersects the null cone of

that point, while spacelike hypersurfaces does not.

There is a strong analogy between 2+1 and 3+1 cases, which suggests that the results can be extended to $n + 1$ dimensions easily. In any dimensions, the solutions can be expressed in terms of spherical waves, $f(r)Y(\Omega)$, where r is the radial distance and Ω denotes the angular part [24]. In addition, to be able to apply the same method, an addition theorem similar to that of the 2+1 and 3+1 dimensions is needed for this higher dimension. The similarity of (3.2.17), (3.2.18) with (3.3.44), (3.3.45) suggests that the solution for higher dimensions are readily given by these equations where the expressions of \bar{B} and \bar{C} in terms of B and C will be found using addition theorems of those dimensions.

REFERENCES

- [1] Friedlander, F. G.: The Wave Equation on a Curved Space-Time, Cambridge University Press, Cambridge, 1975
- [2] Sachs, R. K., Woo, H.: General Relativity for Mathematicians, Springer-Verlag, New York 1977.
- [3] Hawking, S.W., Ellis, G.F.R.: The Large Scale Structure of Space-Time, Cambridge University Press, Cambridge, 1973.
- [4] Kar, S. Sahdev, D.: Scalar Waves in a Wormhole Geometry. Phys. Rev. D 49, 853-861 (1994).
- [5] Bergliaffa E. P., Hibberd, K. E. Electromagnetic Waves in a Wormhole Geometry. Phys. Rev. D62, 044045 (2000)
- [6] Clement, G.: Scattering of Klein-Gordon and Maxwell Waves by an Ellis Geometry. Int. Journ. Theor. Phys. 23 335-350 (1984)
- [7] Esfahani, B. N.: Scattering of Electromagnetic Waves by Static Wormholes. Gen. Rel. Grav. 37 1857 - 1867 (2005)
- [8] Popov, A. A., Sushkov, S. V.: Vacuum polarization of a scalar field in wormhole spacetimes. Phys. Rev. D 63, 044017 (2001)
- [9] Sushkov, S. V., Kim, S.W.: Cosmological Evolution of a Ghost Scalar Field. Gen. Rel. Grav. 36 1671-1678 (2004)
- [10] Lu, H. Q., Shen, L. M., Ji, P., Ji, G. F., Sun, N. J.: The classical wormhole solution and wormhole wavefunction with a nonlinear Born-Infeld scalar field. Int. Journ. Theor. Phys. 42 837-844 (2003)
- [11] Morris, S. M., Thorne, K.S.: Wormholes in Space-Time and Their Use for Interstellar Travel: A Tool for Teaching General relativity. Am. J. Phys. 56, 395-412 (1988)

- [12] Hawking, S. W.: Chronology Protection Conjecture, *Phys. Rev. Lett.* 46, 603-611, (1992).
- [13] Frolov, V. P., Novikov, I. D.: Physical Effects in Wormholes and Time Machines. *Phys. Rev. D* 42, 1057–1065 (1990)
- [14] Konoplya, R. A., Molina, C.: The Ringing Wormholes. *Phys. Rev. D* 71, 124009 (2005)
- [15] Kuhfittig, P. K. F.: Cylindrically Symmetric Wormholes. *Phys. Rev. D* 71, 104007 (2005)
- [16] Visser, M.: *Lorentzian Wormholes: From Einstein to Hawking*. American Institute of Physics, New York (1996)
- [17] Friedman, J. L., Morris, M.S., Novikov, I. D., Echeverria, F., Klinkhammer, G., Thorne, K.S., Yurtsever, U.: Cauchy Problem on Spacetimes with Closed Timelike Curves. *Phys. Rev. D*, 42, 1915-1930, (1990).
- [18] Friedman, J. L., Morris, M.S.: The Cauchy Problem for the Scalar Wave Equation is well defined on a Class of Spacetimes with Closed Timelike Curves. *Phys. Rev. Lett.* 66, 401-404, (1991)
- [19] Friedman, J.L., Morris M.S.: Existence and Uniqueness Theorems for Massless Fields on a Class of Spacetimes with Closed Timelike Curves. *Commun. Math. Phys.* 186, 495-529 (1997).
- [20] Twersky, W.: Multiple Scattering of Radiation by an Arbitrary Configuration of Parallel Cylinders. *J. Acoust. Soc. Am.* 22, 42-46, (1952).
- [21] Hawking, S. W., Israel, W.: *General Relativity: An Einstein Centenary Survey*, Cambridge University Press, 1979.
- [22] Chavel, I.: *Riemannian Geometry: a Modern Introduction*. Cambridge University Press, 1993.

- [23] Küpeli, D. N.: The Method of Separation of Variables for Laplace Beltrami Equation in Semi-Riemannian Geometry, New Developments in Differential Geometry: Proceedings of Colloquium on Differential Geometry, Debrecen, Hungary, July 26-30, 1994. Kluwer Academic Publishers 1994.
- [24] Watson, G. N.: Bessel Functions, Cambridge University Press, London, 1948.
- [25] Gödel, K.: An Example of a New Type of Cosmological Solutions of Einstein's Field Equations of Gravitation. *Rev. Mod. Phys.* 21, 447-450, (1949)
- [26] Hiscock, W. A.: Scalar Perturbations in Gödel's Universe. *Phys. Rev. D* 17, 1497-1500 (1978)
- [27] Bachelot, A: Global Properties of the Wave Equation on Non-globally Hyperbolic Manifolds. *J. Math. Pures Appl.* 81, 35-65, (2002).
- [28] Jackson, J. D.: Classical Electrodynamics, John Wiley & Sons, New York, 1999.
- [29] Heaviside, O.: Electromagnetic theory, Dover Publications, New York, 1950.
- [30] Stratton, J. A.: Electromagnetic Theory, McGraw Hill, New York, 1941.
- [31] Felderhof, B. U., Jones, R.B.: Addition Theorems for Spherical Wave Solutions of the Vector Helmholtz Equation. *J. Math. Phys.* 24, 836-839, (1987).
- [32] Friedman, B., Russek, J.: Addition Theorems for Spherical Waves. *Quart. Appl. Math.* 12, 13-23, (1954).
- [33] Edmonds, A.R.: Angular Momentum in Quantum Mechanics, Princeton University Press, Princeton, 1960.
- [34] Talman, J. D.: Special Functions, A Group Theoretical Approach, W.A. Benjamin Inc., New York, 1968.
- [35] Cramer, J. G., Forward, R. L., Morris, M. S., Visser, M., Benford, G., Landis, G. A.: Natural Wormholes as Gravitational Lenses. *Phys. Rev. D* 51, 3117-3120 (1995)

- [36] Safonova, M., Torres, D. F., Romero, G. E.: Microlensing by Natural Wormholes: Theory and Simulations. *Phys. Rev. D* 65, 023001 (2002).

APPENDIX

CALCULATION OF \bar{A}_{lm} , \bar{B}_{lm} AND \bar{C}_{lm}

Referring to the equations (3.3.33), (3.3.34) and (3.3.35)

$$\begin{aligned}\sum_{lm} A_{lm} \cdot j_l(\omega r) Y_{lm}(\theta, \varphi) &= \sum_{lm} \bar{A}_{lm} j_l(\omega R) Y_{lm}(\Phi, \varphi), \\ \sum_{lm} B_{lm} \cdot h_l^{(1)}(\omega r) Y_{lm}(\theta, \varphi) &= \sum_{lm} \bar{B}_{lm} j_l(\omega r) Y_{lm}(\Phi, \varphi), \\ \sum_{lm} C_{lm} \cdot h_l^{(1)}(\omega R) Y_{lm}(\Phi, \varphi) &= \sum_{lm} \bar{C}_{lm} j_l(\omega r) Y_{lm}(\theta, \varphi),\end{aligned}$$

(3.3.36), (3.3.37) and (3.3.38) can be employed to calculate \bar{A}_{lm} , \bar{B}_{lm} and \bar{C}_{lm} . Considering Ψ_0 ,

$$\begin{aligned}\Psi_0 &= \sum_{lm} A_{lm} \cdot j_l(\omega r) Y_{lm}(\theta, \varphi) = \sum_{lm} A_{lm} \sum_{l'm'} \alpha_{l'm'}^{lm+}(\vec{d}) j_{l'}(\omega R) Y_{l'm'}(\pi - \Theta, \varphi) \\ &= \sum_{lm} A_{lm} \sum_{l'm'} \alpha_{l'm'}^{lm+}(\vec{d}) j_{l'}(\omega R) (-1)^{l'+m'} Y_{l'm'}(\Theta, \varphi) \\ &= \sum_{lm} (-1)^{l+m} \left(\sum_{l'm'} A_{l'm'} \alpha_{lm}^{l'm'+}(\vec{d}) \right) j_l(\omega R) Y_{lm}(\Theta, \varphi).\end{aligned}$$

In the last step the order of summations and indices lm and $l'm'$ are interchanged. It is assumed that these series converge and changing the order of the summations is valid [32].

Thus

$$\bar{A} = (-1)^{l+m} \left(\sum_{l'm'} A_{l'm'} \alpha_{lm}^{l'm'+}(\vec{d}) \right).$$

Calculation of the \bar{B}_{lm} is identical except $\alpha_{lm}^{l'm'+}$ is replaced by $\alpha_{lm}^{l'm'}$. To find C_{lm} :

$$\begin{aligned} \Psi_2 &= \sum_{lm} C_{lm} \cdot h_l^{(1)}(\omega R) Y_{lm}(\Theta, \varphi) = \sum_{lm} (-1)^{l+m} C_{lm} \cdot h_l^{(1)}(\omega R) Y_{lm}(\pi - \Theta, \varphi) \\ &= \sum_{lm} (-1)^{l+m} C_{lm} \sum_{l'm'} \alpha_{l'm'}^{lm}(-\vec{d}) j_{l'}(\omega r) Y_{l'm'}(\theta, \varphi) \\ &= \sum_{lm} \left(\sum_{l'm'} (-1)^{l'+m'} C_{l'm'} \alpha_{lm}^{l'm'}(-\vec{d}) \right) j_l(\omega r) Y_{lm}(\theta, \varphi) \\ &= \sum_{lm} \left(\sum_{l'm'} (-1)^{l'+m'} C_{l'm'} \alpha_{lm}^{l'm'}(-\vec{d}) \right) j_l(\omega r) Y_{lm}(\theta, \varphi). \end{aligned} \tag{4.0.1}$$

Recalling (3.3.39):

$$\begin{aligned} \alpha_{lm}^{l'm'}(-\vec{d}) &= \alpha_{lm}^{l'm}(-\vec{d}) \sum_{\lambda\mu} c(lm|l'm|\lambda 0) h_\lambda^{(1)}(\omega d) Y_{\lambda 0}(\pi, \varphi) \\ &= \sum_{\lambda\mu} c(lm|l'm|\lambda 0) h_\lambda^{(1)}(\omega d) (-1)^\lambda \sqrt{\frac{2\lambda+1}{4\pi}}. \end{aligned}$$

The $\begin{pmatrix} l & l' & \lambda \\ 0 & 0 & 0 \end{pmatrix}$ factor in $c(lm|l'm|\lambda 0)$ is zero when $l' + l + \lambda$ is odd. Thus $(-1)^{l+l'+\lambda} = 1$ and $(-1)^\lambda = (-1)^{l+l'}$, yielding

$$\alpha_{lm}^{l'm'}(-\vec{d}) = (-1)^{l+l'} \sum_{\lambda\mu} c(lm|l'm|\lambda 0) h_\lambda^{(1)}(\omega d) \sqrt{\frac{2\lambda+1}{4\pi}} = (-1)^{l+l'} \alpha_{lm}^{l'm}(\vec{d}).$$

Substituting in (4.0.1)

$$\sum_{lm} C_{lm} \cdot h_l^{(1)}(\omega R) Y_{lm}(\Theta, \varphi) = \sum_{lm} ((-1)^{l+m} \sum_{l'} C_{l'm'} \alpha_{lm}^{l'm}(\vec{d})) j_l(\omega r) Y_{lm}(\theta, \varphi).$$

Hence

$$\bar{C}_{lm} = (-1)^{l+m} \sum_{l'} C_{l'm} \alpha_{lm}^{l'm}(\vec{d}).$$

VITA

Necmi Buğdayc was born in Konya on May 17, 1966. He received his BS degree in Electrical and Electronics engineering from METU in 1988 and his MS degree in Department of Philosophy from METU in 1998. He is running a company producing data acquisition systems for analytical and scientific instruments in METU technopolis.